Structural Engineering and Mechanics, *Vol. 72, No. 4 (2019) 525-540*
DOI: https://doi.org/10.12989/sem.2019.72.4.525

Dynamic instability and free vibration behavior of three-layered soft-cored sandwich beams on nonlinear elastic foundations

Gholamreza Asgari[1a], Gholamhassan Payganeh*[1] and Keramat Malekzadeh Fard[2b]

[1]*Faculty of Mechanical Engineering, Shahid Rajaee Teacher Training University, Tehran, Iran*
[2]*Aerospace Research Institute, Malek Ashtar University of Technology,Tehran, Iran*

(Received March 10, 2019, Revised May 31, 2019, Accepted June 2, 2019)

Abstract. The purpose of the present work was to study the dynamic instability of a three-layered, symmetric sandwich beam subjected to a periodic axial load resting on nonlinear elastic foundation. A higher-order theory was used for analysis of sandwich beams with soft core on elastic foundations. In the higher-order theory, the Reddy's third-order theory was used for the face sheets and quadratic and cubic functions were assumed for transverse and in-plane displacements of the core, respectively. The elastic foundation was modeled as nonlinear's type. The dynamic instability regions and free vibration were investigated for simply supported conditions by Bolotin's method. The results showed that the responses of the dynamic instability of the system were influenced by the excitation frequency, the coefficients of foundation, the core thickness, the dynamic and static load factor. Comparison of the present results with the published results in the literature for the special case confirmed the accuracy of the proposed theory.

Keywords: dynamic instability; natural frequency; nonlinear elastic foundation; mathieu's equation; bolotin's method

1. Introduction

Sandwich structures have been used in many engineering applications since the middle of the 20th century. These structures are characterized by impact and heat resistance, acoustic and vibration reduction and easy assembly. Because of their high strength and stiffness, low weight and durability, these structures are widely used in aerospace, automobile and shipbuilding industries (Doddamani *et al.* 2011 and Cunedioglu 2015). Sandwich structures generally consist of two stiff face sheets and a soft core, which are bonded together. (Frostig *et al.* 1995, 1996, 2004) proposed the higher order sandwich panel theory for investigation of free vibration and bending analyses of sandwich structures. They considered two models for expressing the governing equations of the core. The second model assumed a polynomial description of the displacement fields in the core that was based on the displacement fields of the first model. Frostig and Thomsen (2004) presented a new high-order sandwich plate theory (HSAPT) for the free vibration analysis. In this theory, the cubic and quadratic polynomials were used for in-plane and transverse displacements of the core and CLPT model was used for the face sheets. Analytical solutions were presented for simply supported sandwich plates, but the transverse stress continuity conditions were neglected. (Jam *et al.* 2010) second model of by Frostig and Thomsen (2004) extended by shear deformation theory instead of classical plate theory for the face sheets. The in-plane normal and shear stresses in the core are considered, whereas this solution method not considered by Frostig and Thomsen (2004). (Huang *et al.* 2015) developed the finite element model of a three-layer viscoelastic sandwich beam based on the first-order shear deformation theory and the Hamilton principle. Petras and Sutcliffe (1999) used the higher order sandwich beam theory and studied the bending of sandwich beams. In their theory, the shear stress in thickness directions was assumed to be uniformly distributed; however, a second order function was considered for the vertical displacement of the core. The improved higher order sandwich plate theory, applying the first order shear deformation theory for the face sheets, was introduced by (Malekzadeh *et al.* 2005). Zenkour (2005) presented the comprehensive analysis of FG sandwich plates. The face sheets were assumed to be isotropic and two-constitutional material distribution through the thickness was assumed to vary according to the power law distribution. Bending, buckling, and free vibration of simply supported FG ceramic-metal sandwich plates were also investigated. (Malekzadeh *et al.* 2015) used an improved higher-order sandwich panel theory (IHSAPT) and studied the dynamic response of a sandwich beam with arbitrary cores (foam or functionally graded materials) subjected to single impact at arbitrary impacted face sheet. They used the first-order shear deformation theory for the face sheets and a polynomial description of the displacement fields in the core which was based on the displacement field of the second Frostig's model (Frostig and Thomsen 2004). Malekzadeh Fard (2014) investigated free vibration of a sandwich curved beam with a functionally graded (FG)

*Corresponding author, Associate Professor
E-mail: g.payganeh@sru.ac.ir
[a] Ph.D. Student
[b] Professor

ISSN: 1225-4568 (Print), 1598-6217 (Online)

core. (Bennai *et al.* 2015) developed a new refined hyperbolic shear and normal deformation beam theory is developed to study the free vibration and buckling of functionally graded (FG) sandwich beams under various boundary conditions. (Qin *et al*. 2017, 2018, and 2019) investigated free vibrations of shells with arbitrary boundary conditions. (Huang *et al*. 2015) developed two finite element formulations using different laminate plate theories for the elastic-viscoelastic-elastic sandwich plates. (Safaei *et al.* 2018) investigated the effect of loading frequency on the dynamic behavior of nanocomposite sandwich plates under periodic thermo-mechanical loadings. Fattahi and Safaei (2017) investigated Axial buckling characteristics of nanocomposite beams reinforced by single-walled carbon nanotubes (SWCNTs). They used various types of beam theories namely as Euler---Bernoulli beam theory, Timoshenko beam theory and Reddy beam theory to analyze the buckling behavior of carbon nanotube-reinforced composite beams. Demir (2017) investigated free vibration and damping behaviors of multilayered symmetric sandwich beams and single layered beams made of Functionally Graded Materials investigated, experimentally and numerically.

The classical theory is no longer valid when one uses foam-like core materials (Frostig and Baruch 1990) and hence, a higher order theory is used which takes both the nonlinear displacement fields of the core material and realistic supports into account. Frostig and Baruch (1994) and Frostig (1998) used this theory to study the behavior of a symmetric and non-symmetric sandwich beam with a flexible core. Frostig (1998) developed a theory using the Kirchhoff-Love model (CLPT) for the face sheets and a postulated stress distribution in the core for overall and local buckling analysis of soft core sandwich plates. In many applications, these sandwich structures are subjected to parametric excitation, where a small excitation can produce a large response when the frequency of the excitation is closer to twice the natural frequencies (principal parametric resonance) or combination of different modal frequencies (combination resonances). The investigation about this phenomenon in elastic systems was first studied by Bolotin (1956), who found the dynamic instability regions. The study of parametric instability is well known and can be found in detail in various textbooks, e.g., (Reddy 2004). One may use several methods to study the parametric instability regions. Kar and Sujata (1991) as well as Ray and Kar (1995, 1996) studied the parametric instability regions for simple and combination resonances for different types of sandwich beams with viscoelastic core by using the modified Hsu's procedure. In these works, classical sandwich beam theory was used, and the core was assumed to be rigid in transverse direction. Recently, (Dwivedy *et al.* (2007) studied the dynamic instability regions of a soft-cored sandwich beam using the higher-order theory. (Bremen *et al.* 2001), (Sokolinsky *et al*. 2004), Sokolinsky and Nutt (2004), Yang and Qiao (2005) as well as Liu and Zhao (2006) studied sandwich beams with soft core using the higher-order theory. In all these cases, the study was limited to free vibration analysis of the systems. In many applications, these sandwich structures are subjected to parametric excitation. Unlike the forced vibration in which the resonance occurs only when the excitation frequency is equal to one of the modal frequencies, in case of parametric excitation, a small excitation can produce a large response when the frequency of the excitation is close to twice the natural frequencies (principal parametric resonance) or combination of different modal frequencies (combination resonances). (Ghosh *et al.* 2005) investigated the parametric dynamic stability of an asymmetric sandwich beam with viscoelastic core on viscoelastic supports at the ends and subjected to an axial pulsating load. Smyczynski and Magnucka (2018) analysed the stability of a simply supported five layer sandwich beam subjected to an axial compression. The main goal was to elaborate a mathematical and numerical model of beam.

Mohanty *et al.* 2010 investigated the dynamic stability of functionally graded ordinary beam and functionally graded sandwich beam on Winkler's elastic foundation using finite element method. Effect of elastic foundation and proportional damping on the dynamic instability was analysed by Boss *et al.* 2012. They used the FEM to investigate the dynamic instability of isotropic cantilever and simply supported beams. (Patel *et al.* 1999) analyzed the dynamic instability of laminated composite plates on elastic foundations, using C1 eight-noded shear-flexible plate element. (Pourasghar *et al.* 2015) analysed the dynamic behavior of rotating nanobeam subjected to follower force using the nonlocal elasticity theory. (Pradhan *et al.* 2016) analyzed free vibration of a three layered asymmetric sandwich beam resting on a variable Pasternak foundation subjected to a pulsating axial load by the computational method. (Tornabene *et al.* 2014) presented the static and dynamic analyses of laminated doubly-curved shells and panels of revolution resting on the Winkler-Pasternak elastic foundation. Pourasghar and kamarian (2013) presented the dynamic behavior of a non-uniform column reinforced by single-walled carbon nanotubes resting on an elastic foundation and subjected to follower force. The method of solution was the differential quadrature method. Pourasghar and Chen (2016) presented the investigation of the free vibration response of a carbon nanotube-reinforced cylindrical panel resting on elastic foundation in thermal environments. The response of the elastic medium is formulated by the Winkler/Pasternak model. (Safaei *et al*. 2018) studied the effect of thermal gradient load on natural frequencies of sandwich plates with polymer-based nanocomposite face sheets reinforced by functionally graded (FG) single-walled carbon nanotubes (SWCNTs) agglomerations. They developed First-order shear deformation theory and a moving least square (MLS) shape function based mesh-free method for free vibration and steady state thermal analysis on sandwich plates on two-parameter elastic foundations.

Pourasghar and Chen (2019) used the combined application of the differential quadrature method (DQM) and the Newton-Raphson method to solve the hyperbolic heat conduction equations to obtain temperature, displacements and nonlinear frequency in the functionally graded (FG) nanocomposite Timoshenko microbeam. Moradi-Dastjerdi and Momeni-Khabisi (2018) studied free

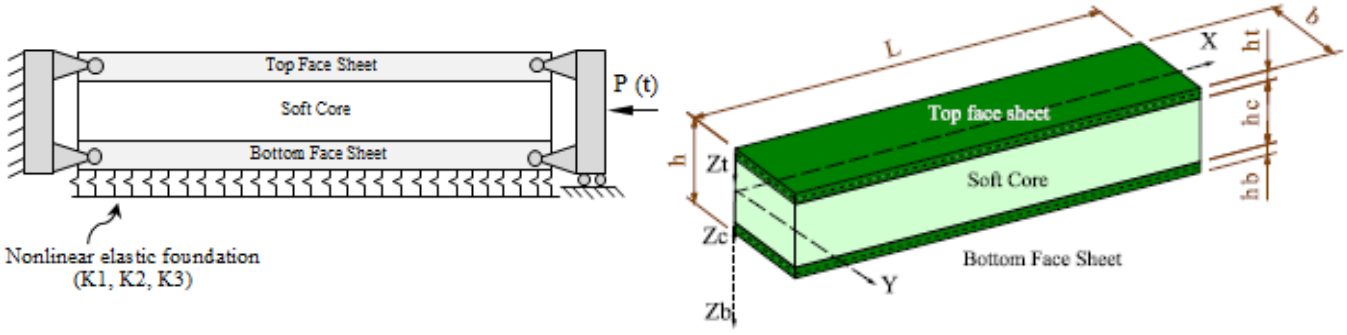

(a) (b)

Fig. 1 (a) Sandwich beam resting on the elastic foundation and subjected to dynamic axial load; (b) Sandwich beam with laminated face sheets along with the coordinates and dimensions of the beam

and forced vibrations, and also resonance and pulse phenomena in sandwich plates based on a mesh-free method and first order shear deformation theory (FSDT). The sandwich plates are resting on Pasternak elastic foundation and subjected to periodic loads. In the equivalent single layer (ESL) theories, transverse stresses are obtained as discontinuous functions at the interface between the layers with different stiffness properties. In layer-wise theories, the number of unknowns depends on the number of the layers and large computational efforts needed. In the present work, an effort was made to develop the governing equation of motion of soft-core sandwich beams using a higher-order theory and Hamilton's principle, and then to obtain the parametric instability regions for different system parameters. In this theory, the Reddy's third-order shear deformable plate theory was used for the face sheets and a polynomial description of the displacement fields in the core was considered, which was based on the displacement field of the second Frostig's model (Frostig and Baruch 1996). The compatibility conditions at the interfaces and the conditions of zero transverse shear stresses on the upper and lower surfaces of the sandwich beam were satisfied. Transverse flexibility as well as transverse normal strain and stress of the core were studied. This study could be highly useful for researchers/designers to suppress vibration and instability using soft-cored sandwich structures.

The purpose of this work was to study the parametric instability of a simply supported sandwich beam with soft-core, subjected to a periodic axial loading resting on nonlinear elastic foundation. Equations of motion were reduced to a set of coupled Mathieu's equations with complex coefficients in the time domain. The regions of instability were obtained by Bolotin's method (Bolotin 1956).

The results obtained from the free vibration and dynamic instability analysis were compared with previous works in the literature. The effects of various parameters were studied on the natural and excitation frequency of the sandwich beams. Moreover, the effects of elastic foundation, static and dynamic load factor, and length to beam thickness ratio upon the zones of instability or excitation frequencies were investigated.

2. Mathematical formulation

A sandwich beam with soft-core and face sheets as dissimilar materials is shown in Fig. 1(a). The beam was hinged at the both ends subjected to a dynamic axial load $P(t) = P_0 + P_t \cos(\Omega t)$, where t is time, P_0 is the static component, P_t is the amplitude of the dynamic component and Ω is the frequency of the applied dynamic load component of $P(t)$. The periodic load P can also be expressed in terms of the linear static buckling load P_{cr} as

$$P(t) = \alpha P_{cr} + \beta P_{cr} \cos \Omega t \qquad (1)$$

where $\alpha = P_0 / P_{cr}$ and $\beta = P_t / P_{cr}$ are termed as the static and dynamic load factors, respectively.

A rectangular sandwich beam with the in-plane dimensions of $L \times b$ and the total thickness of h was considered as shown in Fig. 1(b) (Khalili *et al.* 2015). The coordinates are also shown in this figure. In the following, the indices t and b refer to the top and bottom face sheets of the beam, respectively (Malekzadeh *et al.* 2015). The sandwich beam was considered as simply supported. The sandwich was composed of three layers: the top and bottom face sheets as well as the core layer. All the layers were assumed with uniform thickness and the z coordinate of each layer was measured downward from its mid-plane. The face sheets were generally unequal in thickness, i.e., h_t and h_b were the thicknesses of the top and bottom face sheets, respectively. The face sheets were assumed to be laminated composites. The core was also assumed as a soft material with thickness h_c (Malekzadeh *et al.* 2015).

2.1 Kinematic relations

The mathematical formulations consisted of derivation of the governing equations of motion along with the appropriate boundary conditions for the face sheets and the core through Hamilton's principle. This principle was extremized the Lagrangian consisting of the kinetic energy, strain energy, and external work (Frostig and Baruch 1996). In the present structural model for sandwich beams, the Reddy's third order shear deformable theory was adopted for the face sheets (Malekzadeh Fard *et al.* 2011). Based on

this theory, the displacements u and w of the face sheets in the x (longitudinal) and z (thickness) directions with small linear displacements were expressed through the following relations (Reddy 2004)

$$u_i(x,z,t) = u_0^i(x,t) + z_i\varphi_x^i(x,t) - \frac{4}{3h_i^2}(\varphi_x^i + \frac{\partial w_0^i}{\partial x})z_i^3$$
$$w_i(x,z,t) = w_0^i(x,t) \qquad (i=t,b) \tag{2}$$

where ϕ_x^i (i = t, b) are the rotation components of the transverse normal along the x-axes of the mid-plane of the top and bottom face sheets. Moreover, u_0^i and w_0^i (i=t,b) are displacement component in the x direction and vertical deflection of the top and bottom face sheets, respectively. z_i is the vertical coordinate of each face sheet (i = t, b) and is measured downward from the mid-plane of each face sheet as shown in Fig.1 (b).

The displacement fields were based on the second model of Frostig for the core and a cubic pattern for the in-plane displacements and a quadratic one for the vertical ones can be taken as (Malekzadeh *et al.* 2015)

$$u_c(x,z,t) = u_0^c(x,t) + z_c u_1^c(x,t) + z_c^2 u_2^c(x,t) + z_c^3 u_3^c(x,t)$$
$$w_c(x,z,t) = w_0^c(x,t) + z_c w_1^c(x,t) + z_c^2 w_2^c(x,t) \tag{3}$$

where u_k^c (k = 0, 1, 2, 3) are the unknowns of the in plane displacement components of the core and w_k^c (k = 0, 1,2) are the unknowns of its vertical displacements. Finally, in this model, there were thirteen displacement unknowns. In this study, the core was perfectly bonded to the face sheets. The interface displacement continuity requirements in each face sheet-core interface were defined by (Kheirikhah *et al.* 2011). Moreover, the transverse shear stresses on the upper and lower surfaces of the sandwich beam were zero (Reddy 2004).

2.2 Strains

The kinematic equations for the strains in the face sheets can be defined as

$$\varepsilon_{xx}^i = \varepsilon_{0xx}^i + z_i\varepsilon_{1xx}^i + z_i^3\varepsilon_{3xx}^i$$
$$\varepsilon_{zz}^i = \varepsilon_{yy}^i = \gamma_{xy}^i = \gamma_{zy}^i = 0$$
$$\gamma_{xz}^i = \gamma_{0xz}^i + z_i^2\gamma_{2xz}^i$$
$$\varepsilon_{0xx}^i = u_{0,x}^i, \varepsilon_{1xx}^i = \varphi_{x,x}^i, \varepsilon_{3xx}^i = -\frac{4}{3h_i^2}(\varphi_{x,x}^i + w_{0,xx}^i) \tag{4}$$
$$\gamma_{0xz}^i = \varphi_x^i + w_{0,x}^i, \gamma_{2xz}^i = -\frac{4}{3h_i^2}(\varphi_x^i + w_{0,x}^i)$$

and the strain displacement relations for the core can be expressed as

$$\varepsilon_{xx}^c = \varepsilon_{0xx}^c + z_c\varepsilon_{1xx}^c + z_c^2\varepsilon_{2xx}^c + z_c^3\varepsilon_{3xx}^c$$
$$\varepsilon_{yy}^i = \gamma_{xy}^i = \gamma_{zy}^i = 0 \tag{5}$$
$$\varepsilon_{zz}^c = \varepsilon_{0zz}^c + z_c\varepsilon_{1zz}^c$$
$$\gamma_{xz}^c = \gamma_{0xz}^c + z_c\gamma_{1xz}^c + z_c^2\gamma_{2xz}^c$$
$$\varepsilon_{0xx}^c = u_{0,x}^c, \varepsilon_{1xx}^c = u_{1,x}^c, \varepsilon_{2xx}^c = u_{2,x}^c, \varepsilon_{3xx}^c = u_{3,x}^c$$
$$\varepsilon_{0zz}^c = w_1^c, \varepsilon_{1zz}^c = 2w_2^c$$
$$\gamma_{0xz}^i = u_1^c + w_{0,x}^c, \gamma_{1xz}^c = 2u_2^c + w_{1,x}^c, \gamma_{2xz}^c = 3u_3^c + w_{2,x}^c$$

The compatibility conditions were presented by assuming perfect bonding between the core and face sheets (Kheirikhah *et al.* 2011)

$$u_c(z_c = -\frac{h_c}{2}) = u_t(z_t = \frac{h_t}{2})$$
$$u_c(z_c = \frac{h_c}{2}) = u_b(z_b = -\frac{h_b}{2})$$
$$w_c(z_c = -\frac{h_c}{2}) = w_t(z_t = \frac{h_t}{2}) \tag{6}$$
$$w_c(z_c = \frac{h_c}{2}) = w_b(z_b = -\frac{h_b}{2})$$

Using the displacement fields of the core Eqs. (3) and (2) and some simplifications, the compatibility conditions from Eq. (6) can be written as

$$u_0^t = u_0^c - \frac{h_c}{2}u_1^c + \frac{h_c^2}{4}u_2^c - \frac{h_c^3}{8}u_3^c - \frac{h_t}{3}\phi_x^t + \frac{h_t}{6}w_{0,x}^t$$
$$u_0^b = u_0^c + \frac{h_c}{2}u_1^c + \frac{h_c^2}{4}u_2^c + \frac{h_c^3}{8}u_3^c + \frac{h_b}{3}\phi_x^b - \frac{h_b}{6}w_{0,x}^b$$
$$w_0^t = w_0^c - \frac{h_c}{2}w_1^c + \frac{h_c^2}{4}w_2^c \tag{7}$$
$$w_0^b = w_0^c + \frac{h_c}{2}w_1^c + \frac{h_c^2}{4}w_2^c$$

It can be seen from Eq. (7) that the number of unknowns in the core and face sheets was reduced to seven and two, respectively. These unknowns were $u_0^c, u_1^c, u_2^c, u_3^c, w_0^c, w_1^c, w_2^c$, ϕ_x^t and ϕ_x^b.

2.3. Governing equations

The equations of motion for the face sheets and the core were derived through the principle of the minimum potential energy:

$$\int_{t_1}^{t_2}\delta L dt = \int_{t_1}^{t_2}(\delta U - \delta T + \delta W_{ext})dt = 0 \tag{8}$$

where T is the kinetic energy, W_{ext} is the external work energy, U is the strain energy, t is the time coordinate between the times t_1 and t_2, and δ denotes the variation operator. The first variation of the internal potential energy for the sandwich beam is:

$$\delta U = \int_{v_t}(\sigma_{xx}^t\delta\varepsilon_{xx}^t + \tau_{xz}^t\delta\gamma_{xz}^t)dV_t + \int_{v_b}(\sigma_{xx}^b\delta\varepsilon_{xx}^b + \tau_{xz}^b\delta\gamma_{xz}^b)dV_b + \int_{v_t}(\sigma_{zz}^c\delta\varepsilon_{zz}^c + \tau_{xz}^c\delta\gamma_{xz}^c + \sigma_{xx}^c\delta\varepsilon_{xx}^c)dV_c \tag{9}$$
$$dV_i = dA_i dz_i = dx_i dz_i, \qquad (i = t,b,c)$$

where σ_{ii} and ε_{ii} (i = x) are the normal stresses and strains in the x direction, respectively; the superscripts t and b correspond, respectively, to the top and bottom face sheets; τ_{iz}^{c} and γ_{iz}^{c} (i = x) are the vertical shear stresses and strains in the core, respectively; σ_{zz}^{c} and τ_{xz}^{c} are the normal and shear stresses in the core, respectively; σ_{xx}^{c} is plane normal stress in the x direction of the core; V_t , V_b , and V_c are the volumes of the top and bottom face sheets as well as the core, respectively. The first variation of the kinetic energy, upon assuming the homogeneous conditions for the displacement and velocity with respect to the time coordinate, is:

$$\delta T=\int_{t_1}^{t_2}\left[\begin{array}{l}\int_0^L\int_{-\frac{h_t}{2}}^{-\frac{h_t}{2}}\rho_t(\ddot{u}_{0t}\delta u_{ot}+\ddot{w}_{0t}\delta w_{ot})dxdz\\ +\int_0^L\int_{-\frac{h_b}{2}}^{-\frac{h_b}{2}}\rho_b(\ddot{u}_{0b}\delta u_{ob}+\ddot{w}_{0b}\delta w_{ob})dxdz\\ +\int_0^L\int_{-\frac{h_c}{2}}^{-\frac{h_c}{2}}\rho_c(\ddot{u}_c\delta u_c+\ddot{w}_c\delta w_c)dxdz\end{array}\right]dt \qquad (10)$$

where ρ_t , ρ_b and ρ_c are the densities of the bottom face sheet, top face sheet, and core, respectively. In all the cases, the u component was horizontal while the w component was vertical. Moreover, (..) denoted the second time derivative. The variation of the external work is:

$$\delta W_{ext}=-\int_0^L F_s\delta w_0dx-(1/2)\left(\delta\int_0^L\overline{P}(t)(w_{t,x}^2+w_{b,x}^2)dx\right) \qquad (11)$$

where $F_s=-K_1w_0+K_2w_{0,xx}-K_3w_0^3$; K_1 $\left(N/m^2\right)$ and K_3 $\left(N/m^4\right)$ are linear and nonlinear coefficients of elastic foundation, respectively and K_2 (N) is the coefficient of shear stiffness of the elastic foundation. Here $w_{t,x}=\partial w_t/\partial x$ and $w_{b,x}=\partial w_b/\partial x$. The stress resultants for the two face sheets and the core (i= t, b, c) can be defined as:

$$\begin{aligned}\left\{N_{xx}^i\ M_{xx}^i\ P_{xx}^i\ S_{xx}^i\right\}^T&=\int_{-h_i/2}^{h_i/2}\left[\sigma_{xx}^i\right]\left\{1\ z_i\ z_i^2\ z_i^3\right\}^T dz_i,\\ \left\{N_{zz}^i\ M_{zz}^i\ P_{zz}^i\ S_{zz}^i\right\}^T&=\int_{-h_i/2}^{h_i/2}\left[\sigma_{zz}^i\right]\left\{1\ z_i\ z_i^2\ z_i^3\right\}^T dz_i,\\ \left\{Q_{xz}^i\ M_{xz}^i\ P_{xz}^i\ S_{xz}^i\right\}^T&=\int_{-h_i/2}^{h_i/2}\left[\tau_{xz}^i\right]\left\{1\ z_i\ z_i^2\ z_i^3\right\}^T dz_i,\end{aligned} \qquad (12)$$

Using Hamilton's principle (Eqs. (9)-(11)) and kinematic relations (Eqs. (2)-(6) and (8)), the equations of motion can be obtained as:

$$\begin{aligned}&-(\frac{dN_{xx}^{\ t}}{dx}+\frac{dN_{xx}^{\ c}}{dx}+\frac{dN_{xx}^{\ b}}{dx})+(I_0^{\ t}+I_0^{\ b}+I_0^{\ c})\ddot{u}_0^c+\\ &(-\frac{h_c}{2}I_0^{\ t}+\frac{h_c}{2}I_0^{\ b}+I_1^{\ c})\ddot{u}_1^{\ c}+(\frac{h_c^2}{4}I_0^{\ t}+\frac{h_c^2}{4}I_0^{\ b}+I_2^{\ c})\ddot{u}_2^c+\\ &(-\frac{h_c^{\ 3}}{8}I_0^{\ t}+\frac{h_c^3}{8}I_0^{\ b}+I_3^{\ c})\ddot{u}_3^{\ c}+(I_1^{\ t}-\frac{h_t}{3}I_0^{\ t}-\frac{4}{3h_t^2}I_3^t)\ddot{\varphi}_x^{\ t}+\\ &(\frac{h_t}{6}I_0^{\ t}-\frac{4}{3h_t^2}I_3^t-\frac{h_b}{6}I_0^{\ b}-\frac{4}{3h_b^2}I_3^b)\ddot{w}_{0,x}^c+(I_1^{\ b}+\frac{h_b}{3}I_0^{\ b}-\\ &\frac{4}{3h_b^2}I_3^b)\ddot{\varphi}_x^{\ b}+(-\frac{h_ch_t}{12}I_0^{\ t}+\frac{2h_c}{3h_t^2}I_3^t+\frac{h_ch_b}{12}I_0^b+\\ &\frac{2h_c}{3h_b^2}I_3^b)\ddot{w}_{1,x}^{\ c}+(\frac{h_c^2h_t}{24}I_0^t-\frac{h_c^2}{3h_t^2}I_3^t-\frac{h_c^2h_b}{24}I_0^b\\ &-\frac{h_c^2}{3h_b^2}I_3^b)\ddot{w}_{2,x}^{\ c}=0\end{aligned} \qquad (13)$$

$$\begin{aligned}&\frac{h_c}{2}\frac{dN_{xx}^{\ t}}{dx}-\frac{h_c}{2}\frac{dN_{xx}^{\ b}}{dx}-\frac{dM_{xx}^{\ c}}{dx}+Q_x^c+(-\frac{h_c}{2}I_0^{\ t}+\frac{h_c}{2}I_0^{\ b}\\ &+I_1^{\ c})\ddot{u}_0^c+(\frac{h_c^2}{4}I_0^{\ t}+\frac{h_c^2}{4}I_0^{\ b}+I_2^{\ c})\ddot{u}_1^{\ c}+(-\frac{h_c^3}{8}I_0^{\ t}+\frac{h_c^3}{8}I_0^{\ b}\\ &+I_3^{\ c})\ddot{u}_2^c+(\frac{h_c^4}{16}I_0^{\ t}+\frac{h_c^4}{16}I_0^{\ b}+I_4^{\ c})\ddot{u}_3^{\ c}+(\frac{h_ch_t}{6}I_0^{\ t}-\frac{h_c}{2}I_1^t\\ &+\frac{2h_c}{3h_t^2}I_3^t)\ddot{\varphi}_x^{\ t}+(\frac{h_ch_b}{6}I_0^b+\frac{h_c}{2}I_1^{\ b}-\frac{2h_c}{3h_b^2}I_3^b)\ddot{\varphi}_x^{\ b}+\\ &(-\frac{h_ch_t}{12}I_0^{\ t}+\frac{2h_c}{3h_t^2}I_3^t-\frac{h_ch_b}{12}I_0^{\ b}+\frac{2h_c}{3h_b^2}I_3^b)\ddot{w}_{0,x}^c+(\frac{h_c^2h_t}{24}I_0^{\ t}\\ &-\frac{h_c^2}{3h_t^2}I_3^t+\frac{h_c^2h_b}{24}I_0^b+\frac{h_c^2}{3h_b^2}I_3^b)\ddot{w}_{1,x}^{\ c}+(-\frac{h_c^3h_t}{48}I_0^t+\frac{h_c^3}{6h_t^2}I_3^t\\ &-\frac{h_c^3h_b}{48}I_0^b-\frac{h_c^3}{6h_b^2}I_3^b)\ddot{w}_{2,x}^{\ c}=0\end{aligned} \qquad (14)$$

$$\begin{aligned}&-\frac{h_c^{\ 2}}{4}\frac{dN_{xx}^{\ t}}{dx}-\frac{h_c^{\ 2}}{4}\frac{dN_{xx}^{\ b}}{dx}-\frac{dP_{xx}^{\ c}}{dx}+2M_{xz}^c+(\frac{h_c^2}{4}I_0^{\ t}\\ &+\frac{h_c^2}{4}I_0^{\ b}+I_2^{\ c})\ddot{u}_0^c+(-\frac{h_c^3}{8}I_0^{\ t}+\frac{h_c^3}{8}I_0^{\ b}+I_3^{\ c})\ddot{u}_1^{\ c}\\ &+(\frac{h_c^4}{16}I_0^{\ t}+\frac{h_c^4}{16}I_0^{\ b}+I_4^{\ c})\ddot{u}_2^c+(-\frac{h_c^{\ 5}}{32}I_0^{\ t}+\frac{h_c^5}{32}I_0^{\ b}\\ &+I_5^{\ c})\ddot{u}_3^{\ c}+(-\frac{h_c^2h_t}{12}I_0^{\ t}+\frac{h_c^2}{4}I_1^{\ t}-\frac{h_c^2}{3h_t^2}I_3^t)\ddot{\varphi}_x^{\ t}\\ &+(\frac{h_c^2h_b}{12}I_0^{\ b}+\frac{h_c^2}{4}I_1^{\ b}-\frac{h_c^2}{3h_b^2}I_3^b)\ddot{\varphi}_x^{\ b}+(\frac{h_c^2h_t}{24}I_0^{\ t}\\ &-\frac{h_c^2}{3h_t^2}I_3^t-\frac{h_c^2h_b}{24}I_0^{\ b}-\frac{h_c^2}{3h_b^2}I_3^b)\ddot{w}_{0,x}^c+(-\frac{h_c^3h_t}{48}I_0^{\ t}+\frac{h_c^3}{6h_t^2}I_3^t\\ &-\frac{h_c^3h_b}{48}I_0^b-\frac{h_c^3}{6h_b^2}I_3^b)\ddot{w}_{1,x}^{\ c}+(\frac{h_c^4h_t}{96}I_0^t-\frac{h_c^4}{12h_t^2}I_3^t\\ &-\frac{h_c^4h_b}{96}I_0^b-\frac{h_c^4}{12h_b^2}I_3^b)\ddot{w}_{2,x}^{\ c}=0\end{aligned} \qquad (15)$$

$$\begin{aligned}&\frac{h_c^3}{8}\frac{dN_{xx}^{\ t}}{dx}-\frac{h_c^3}{8}\frac{dN_{xx}^{\ b}}{dx}-\frac{dS_{xx}^{\ c}}{dx}+3P_{xz}^c+(-\frac{h_c^3}{8}I_0^{\ t}+\frac{h_c^3}{8}I_0^{\ b}\\ &+I_3^{\ c})\ddot{u}_0^c+(\frac{h_c^4}{16}I_0^{\ t}+\frac{h_c^4}{16}I_0^{\ b}+I_4^{\ c})\ddot{u}_1^{\ c}+(-\frac{h_c^5}{32}I_0^{\ t}+\frac{h_c^5}{32}I_0^{\ b}\\ &+I_5^{\ c})\ddot{u}_2^c+(\frac{h_c^6}{64}I_0^{\ t}+\frac{h_c^6}{64}I_0^{\ b}+I_6^{\ c})\ddot{u}_3^{\ c}+(\frac{h_c^3h_t}{24}I_0^{\ t}-\frac{h_c^3}{8}I_1^t\\ &+\frac{h_c^3}{6h_t^2}I_3^t)\ddot{\varphi}_x^{\ t}+(\frac{h_c^3h_b}{24}I_0^{\ b}+\frac{h_c^3}{8}I_1^{\ b}-\frac{h_c^3}{3h_b^2}I_3^b)\ddot{\varphi}_x^{\ b}+\\ &(-\frac{h_c^3h_t}{48}I_0^{\ t}+\frac{h_c^3}{6h_t^2}I_3^t-\frac{h_c^3h_b}{48}I_0^{\ b}-\frac{h_c^3}{6h_b^2}I_3^b)\ddot{w}_{0,x}^c+(\frac{h_c^4h_t}{96}I_0^{\ t}\\ &+\frac{h_c^4}{12h_t^2}I_3^t+\frac{h_c^4h_b}{96}I_0^b+\frac{h_c^4}{12h_b^2}I_3^b)\ddot{w}_{1,x}^{\ c}+(-\frac{h_c^5h_t}{192}I_0^t\\ &+\frac{h_c^5}{24h_t^2}I_3^t-\frac{h_c^5h_b}{192}I_0^b-\frac{h_c^5}{24h_b^2}I_3^b)\ddot{w}_{2,x}^{\ c}=0\end{aligned} \qquad (16)$$

$$\frac{h_t}{3}\frac{dN_{xx}{}^{t}}{dx}-\frac{dM_{xx}{}^{t}}{dx}+\frac{4}{3h_t^2}\frac{dS_{xx}{}^{t}}{dx}+Q_{xz}^{t}-\frac{4}{h_t^2}P_{xz}^{t}+(I_1{}^{t}-\frac{h_t}{3}I_0{}^{t})\ddot{u}_0^c+(-\frac{h_c}{2}I_1{}^{t}+\frac{h_ch_t}{6}I_0{}^{t})\ddot{u}_1^c+(\frac{h_c^2}{4}I_1{}^{t}-\frac{h_th_c^2}{12}I_0{}^{t})\ddot{u}_2^c+(-\frac{h_c^3}{8}I_1{}^{t}+\frac{h_th_c^3}{24}I_0{}^{t})\ddot{u}_3{}^{c}+(-\frac{2h_t}{3}I_1{}^{t}+I_2^t+\frac{h_t^2}{9}I_0{}^{t}-\frac{4}{3h_t^2}I_4^t+\frac{4}{9h_t}I_3^t-\frac{4}{3h_t^2}I_3^t+I_4^t-\frac{4}{3h_t^2}I_6^t)\ddot{\varphi}_x{}^{t}+(-\frac{h_t^2}{18}I_0{}^{t}+\frac{h_t}{6}I_1^t-\frac{4}{3h_t^2}I_4^t+\frac{2}{9h_t}I_3^t+\frac{16}{9h_t^4}I_6^t)\ddot{w}_{0,x}^c+(-\frac{h_ch_t}{12}I_1{}^{t}+\frac{2h_c}{3h_t^2}I_4^t+\frac{h_ch_t^2}{36}I_0^t-\frac{h_c}{9h_t}I_3^t-\frac{8h_c}{9h_t^4}I_6^t)\ddot{w}_{1,x}{}^{c}+(\frac{h_c^2h_t}{24}I_1{}^{t}-\frac{h_c^2}{3h_t^2}I_4^t-\frac{h_c^2h_t^2}{72}I_0^t+\frac{h_c^2}{18h_t}I_3^t+\frac{4h_c^2}{9h_t^4}I_6^t)\ddot{w}_{2,x}{}^{c}=0 \tag{17}$$

$$-\frac{h_b}{3}\frac{dN_{xx}{}^{b}}{dx}-\frac{dM_{xx}{}^{b}}{dx}+\frac{4}{3h_b^2}\frac{dS_{xx}{}^{b}}{dx}+Q_{xz}^{b}-\frac{4}{h_b^2}P_{xz}^{b}+(I_1{}^{b}+\frac{h_b}{3}I_0{}^{b})\ddot{u}_0^c+(\frac{h_c}{2}I_1{}^{b}+\frac{h_ch_b}{6}I_0{}^{b})\ddot{u}_1{}^{c}+(\frac{h_c^2}{4}I_1{}^{b}+\frac{h_bh_c^2}{12}I_0{}^{b})\ddot{u}_2^c+(\frac{h_c^3}{8}I_1{}^{b}+\frac{h_bh_c^3}{24}I_0{}^{b})\ddot{u}_3{}^{c}+(\frac{2h_b}{3}I_1{}^{b}+I_2^b+\frac{h_b^2}{9}I_0{}^{b}-\frac{4}{3h_b^2}I_4^b-\frac{4}{9h_b}I_3^b-\frac{4}{3h_b^2}I_3^b+I_4^b-\frac{4}{3h_b^2}I_6^b)\ddot{\varphi}_x{}^{b}+(-\frac{h_b^2}{18}I_0{}^{b}-\frac{h_b}{6}I_1^b-\frac{4}{3h_b^2}I_4^b-\frac{2}{9h_b}I_3^b+\frac{16}{9h_b^4}I_6^b)\ddot{w}_{0,x}^c+(\frac{h_ch_b}{12}I_1{}^{b}+\frac{2h_c}{3h_b^2}I_4^b+\frac{h_ch_b^2}{36}I_0^b+\frac{h_c}{9h_b}I_3^b-\frac{8h_c}{9h_b^4}I_6^b)\ddot{w}_{1,x}{}^{c}+(-\frac{h_c^2h_b}{24}I_1{}^{t}-\frac{h_c^2}{3h_b^2}I_4^b-\frac{h_c^2h_b^2}{72}I_0^b+\frac{h_c^2}{18h_b}I_3^b)\ddot{w}_{2,x}{}^{c}=0 \tag{18}$$

$$\frac{h_t}{6}\frac{d^2N_{xx}^t}{dx^2}-\frac{4}{3h_t^2}\frac{d^2S_{xx}^t}{dx^2}-\frac{h_b}{6}\frac{d^2N_{xx}^b}{dx^2}+\frac{4}{3h_b^2}\frac{d^2S_{xx}^b}{dx^2}-\frac{dQ_x^t}{dx}-\frac{dQ_x^b}{dx}-\frac{dQ_x^c}{dx}+\frac{4}{h_t^2}\frac{dP_{xz}^t}{dx}+\frac{4}{h_b^2}\frac{dP_{xz}^b}{dx}+K_2(w_0^c+\frac{h_c}{2}w_1^c+\frac{h_c^2}{4}w_2^c)-K_2(w_{0,xx}^c+\frac{h_c}{2}w_{1,xx}^c+\frac{h_c^2}{4}w_2^c)+K_3(w_0^{c3}+\frac{3h_c^5}{32}w_1^cw_2^{c2}+\frac{3h_c^4}{16}w_0^cw_2^{c2}+\frac{3h_c^4}{16}w_2^cw_1^{c2}+\frac{3h_c^3}{4}w_0^cw_1^cw_2^c+\frac{3h_c^2}{4}w_2^cw_0^{c2}+\frac{3h_c^2}{4}w_0^cw_1^{c2}+\frac{3h_c}{2}w_1^cw_0^{c2}+\frac{h_c^3}{8}w_1^{c3}+\frac{h_c^6}{64}w_2^{c3})+\bar{P}(t)(2w_{0,xx}^c+\frac{h_c^2}{2}w_{2,xx}^c)+(-\frac{h_t}{6}I_0^t+\frac{4}{3h_t^2}I_3^t+\frac{h_b}{6}I_0^b+\frac{4}{3h_b^2}I_3^b)\ddot{u}_{0,x}^c+(\frac{h_ch_t}{12}I_0^t-\frac{2h_c}{3h_t^2}I_3^t+\frac{h_ch_b}{12}I_0^b+\frac{2h_c}{3h_b^2}I_3^b)\ddot{u}_{1,x}^c+(-\frac{h_c^2h_t}{24}I_0^t+\frac{h_c^2}{3h_t^2}I_3^t+\frac{h_c^2h_b}{24}I_0^b+\frac{h_c^2}{3h_b^2}I_3^b)\ddot{u}_{2,x}^c+(\frac{h_c^3h_t}{48}I_0^t-\frac{h_c^3}{6h_t^2}I_3^t+\frac{h_c^3h_b}{48}I_0^b+\frac{h_c^3}{6h_b^2}I_3^b)\ddot{u}_{3,x}^c+(\frac{h_b}{6}I_1^b+\frac{h_b^2}{18}I_0^b+\frac{4}{3h_b^2}I_4^b+\frac{2}{9h_b}I_3^b-\frac{16}{9h_b^4}{}^{b}{}_{6})\ddot{\varphi}_{x,x}^b+(-\frac{h_t}{6}I_1^t+\frac{h_t^2}{18}I_0^t+\frac{4}{3h_t^2}I_4^t-\frac{2}{9h_t}I_3^t-\frac{16}{9h_t^4}I_6^t)\ddot{\varphi}_{x,x}^t+(-\frac{h_t^2}{36}I_0^t+\frac{4}{9h_t}I_3^t-\frac{16}{9h_t^4}I_6^t-\frac{h_b^2}{36}I_0^b-\frac{4}{9h_b}I_3^b+\frac{16}{9h_b^4}I_6^b)\ddot{w}_{0,xx}^c+(\frac{h_ch_b^2}{72}I_0^b+\frac{2h_c}{9h_b}I_3^b+\frac{8h_c}{9h_b^4}I_6^b+\frac{h_ch_t^2}{72}I_0^t-\frac{2h_c}{9h_t}I_3^t+\frac{8h_c}{9h_t^4}I_6^t)\ddot{w}_{0,xx}^c+(-\frac{h_c^2h_t}{144}I_0^t+\frac{h_c^2}{9h_t}I_3^t-\frac{4h_c^2}{9h_t^4}I_6^t-\frac{h_c^2h_b^2}{144}I_0^b-\frac{h_c^2}{9h_b}I_3^b-\frac{4h_c^2}{9h_b^4}I_6^b)\ddot{w}_{1,xx}^c+(\frac{h_c^3h_t}{288}I_0^t-\frac{h_c^3}{18h_t}I_3^t+\frac{2h_c^3}{9h_t^4}I_6^t+\frac{h_c^3h_b^2}{288}I_0^b+\frac{h_c^3}{18h_b}I_3^b+\frac{2h_c^3}{9h_b^4}I_6^b)\ddot{w}_{2,xx}^c+(-\frac{h_c}{2}I_0^t+\frac{h_c}{2}I_0^b+I_1^c)\ddot{w}_0^c+(\frac{h_c^2}{4}I_0^t+\frac{h_c^2}{4}I_0^b+I_2^c)\ddot{w}_1^c+(-\frac{h_c^3}{8}I_0^t+\frac{h_c^3}{8}I_0^b+I_3^c)\ddot{w}_2^c=0 \tag{19}$$

$$-\frac{h_ch_t}{12}\frac{d^2N_{xx}^t}{dx^2}+\frac{2h_c}{3h_t^2}\frac{d^2S_{xx}^t}{dx^2}+\frac{h_ch_b}{12}\frac{d^2N_{xx}^b}{dx^2}-\frac{2h_c}{3h_b^2}\frac{d^2S_{xx}^b}{dx^2}+\frac{h_c}{2}\frac{dQ_x^t}{dx}-\frac{h_c}{2}\frac{dQ_x^b}{dx}-\frac{dM_{xz}^c}{dx}-\frac{2h_c}{h_b^2}\frac{dP_{xz}^b}{dx}-\frac{2h_c}{h_t^2}\frac{dP_{xz}^t}{dx}+N_{zz}^c+K_1(\frac{h_c}{2})(w_0^c+\frac{h_c}{2}w_1^c+\frac{h_c^2}{4}w_2^c)-K_2(\frac{h_c}{2})(w_{0,xx}^c+\frac{h_c}{2}w_{1,xx}^c+\frac{h_c^2}{4}w_{2,xx}^c)+K_3(\frac{h_c}{2})(w_0^{c3}+\frac{3h_c^5}{32}w_1^cw_2^{c2}+\frac{3h_c^4}{16}w_0^cw_2^{c2}+\frac{3h_c^4}{16}w_2^cw_1^{c2}+\frac{3h_c^3}{4}w_0^cw_1^cw_2^c+\frac{3h_c^2}{4}w_2^cw_0^{c2}+\frac{3h_c^2}{4}w_0^cw_1^{c2}+\frac{3h_c}{2}w_1^cw_0^{c2}+\frac{h_c^3}{8}w_1^{c3}+\frac{h_c^6}{64}w_2^{c3})+\bar{P}(t)(\frac{h_c^2}{2}w_{1,xx}^c)+(\frac{h_ch_t}{12}I_0^t-\frac{2h_c}{3h_t^2}I_3^t-\frac{h_ch_b}{12}I_0^b-\frac{2h_c}{3h_b^2}I_3^b)\ddot{u}_{0,x}^c+(-\frac{h_c^2h_t}{24}I_0^t+\frac{h_c^2}{3h_t^2}I_3^t+\frac{h_c^2h_b}{24}I_0^b-\frac{h_c^2}{3h_b^2}I_3^b)\ddot{u}_{1,x}^c+(\frac{h_c^3h_t}{48}I_0^t-\frac{h_c^3}{6h_t^2}I_3^t-\frac{h_c^3h_b}{48}I_0^b+\frac{h_c^3}{6h_b^2}I_3^b)\ddot{u}_{2,x}^c+(-\frac{h_c^4h_t}{96}I_0^t+\frac{h_c^4}{12h_t^2}I_3^t-\frac{h_c^4h_b}{96}I_0^b-\frac{h_c^4}{12h_b^2}I_3^b)\ddot{u}_{3,x}^c+(-\frac{h_ch_b}{12}I_1^b-\frac{h_ch_b^2}{36}I_0^b-\frac{2h_c}{3h_b^2}I_4^b-\frac{h_c}{9h_b}I_3^b+\frac{32h_c}{36h_b^4}I_6^b)\ddot{\varphi}_{x,x}^b+(\frac{h_ch_t}{12}I_1^t-\frac{h_ch_t^2}{36}I_0^t-\frac{2h_c}{3h_t^2}I_4^t+\frac{h_c}{9h_t}I_3^t+\frac{32h_c}{36h_t^4}I_6^t)\ddot{\varphi}_{x,x}^t+(\frac{h_ch_t^2}{72}I_0^t-\frac{2h_c}{9h_t}I_3^t+\frac{8h_c}{9h_t^4}I_6^t+\frac{h_ch_b^2}{72}I_0^b+\frac{2h_c}{9h_b}I_3^b+\frac{8h_c}{9h_t^4}I_6^b)\ddot{w}_{0,xx}^c+(-\frac{h_c^2h_t^2}{144}I_0^t+\frac{h_c^2}{9h_t}I_3^t-\frac{4h_c^2}{9h_t^4}I_6^t-\frac{h_c^2h_b^2}{144}I_0^b-\frac{h_c^2}{9h_b}I_3^b-\frac{4h_c^2}{9h_b^4}I_6^b)\ddot{w}_{1,xx}^c+(\frac{h_c^3h_t^2}{288}I_0^t-\frac{h_c^3}{18h_t}I_3^t+\frac{2h_c^3}{9h_t^4}I_6^t+\frac{h_c^3h_b^2}{288}I_0^b+\frac{h_c^3}{18h_b}I_3^b+\frac{2h_c^3}{9h_b^4}I_6^b)\ddot{w}_{2,xx}^c+(-\frac{h_c}{2}I_0^t+\frac{h_c}{2}I_0^b+I_1^c)\ddot{w}_0^c+(\frac{h_c^2}{4}I_0^t+\frac{h_c^2}{4}I_0^b+I_2^c)\ddot{w}_1^c+(-\frac{h_c^3}{8}I_0^t+\frac{h_c^3}{8}I_0^b+I_3^c)\ddot{w}_2^c=0 \tag{20}$$

$$\frac{h_c^2h_t}{24}\frac{d^2N_{xx}^t}{dx^2}-\frac{h_c^2}{3h_t^2}\frac{d^2S_{xx}^t}{dx^2}-\frac{h_c^2h_b}{24}\frac{d^2N_{xx}^b}{dx^2}+\frac{h_c^2}{3h_b^2}\frac{d^2S_{xx}^b}{dx^2}-\frac{h_c^2}{4}\frac{dQ_x^t}{dx}-\frac{h_c^2}{4}\frac{dQ_x^b}{dx}-\frac{dP_{xz}^c}{dx}+\frac{h_c^2}{h_b^2}\frac{dP_{xz}^b}{dx}+\frac{h_c^2}{h_t^2}\frac{dP_{xz}^t}{dx}+2M_{zz}^c+K_1(\frac{h_c^2}{4})(w_0^c+\frac{h_c}{2}w_1^c+\frac{h_c^2}{4}w_2^c)-K_2(\frac{h_c^2}{4})(w_{0,xx}^c+\frac{h_c}{2}w_{1,xx}^c+\frac{h_c^2}{4}w_{2,xx}^c)+K_3(\frac{h_c^2}{4})(w_0^{c3}+\frac{3h_c^5}{32}w_1^cw_2^{c2}+\frac{3h_c^4}{16}w_0^cw_2^{c2}+\frac{3h_c^4}{16}w_2^cw_1^{c2}+\frac{3h_c^3}{4}w_0^cw_1^cw_2^c+\frac{3h_c^2}{4}w_2^cw_0^{c2}+\frac{3h_c^2}{4}w_0^cw_1^{c2}+\frac{3h_c}{2}w_1^cw_0^{c2}+\frac{h_c^3}{8}w_1^{c3}+\frac{h_c^6}{64}w_2^{c3})+\bar{P}(t)(\frac{h_c^2}{2}w_{0,xx}^c+\frac{h_c^4}{8}w_{2,xx}^c) \tag{21}$$

$$+(-\frac{h_c^2 h_t}{24} I_0^t + \frac{h_c^2}{3h_t^2} I_3^t + \frac{h_c^2 h_b}{24} I_0^b + \frac{h_c^2}{3h_b^2} I_3^b)\ddot{u}_{0,x}^c + (\frac{h_c^3 h_t}{48} I_0^t$$
$$-\frac{h_c^3}{6h_t^2} I_3^t + \frac{h_c^3 h_b}{48} I_0^b + \frac{h_c^3}{6h_b^2} I_3^b)\ddot{u}_{1,x}^c + (-\frac{h_c^4 h_t}{96} I_0^t + \frac{h_c^4}{12h_t^2} I_3^t$$
$$+\frac{h_c^4 h_b}{96} I_0^b + \frac{h_c^4}{12h_b^2} I_3^b)\ddot{u}_{2,x}^c + (\frac{h_c^5 h_t}{192} I_0^t - \frac{h_c^5}{24h_t^2} I_3^t + \frac{h_c^5 h_b}{192} I_0^b$$
$$+\frac{h_c^5}{24h_b^2} I_3^b)\ddot{u}_{3,x}^c + (\frac{h_c^2 h_b}{24} I_1^b + \frac{h_c^2 h_b^2}{72} I_0^b + \frac{h_c^2}{3h_b^2} I_4^b + \frac{h_c^2}{18h_b} I_3^b$$
$$-\frac{32h_c^2}{72h_b^4} I_6^b)\ddot{\varphi}_{x,x}^b + (-\frac{h_c^2 h_t}{24} I_1^t + \frac{h_c^2 h_t^2}{72} I_0^t + \frac{h_c^2}{3h_t^2} I_4^t - \frac{h_c^2}{18h_t} I_3^t$$
$$-\frac{32h_c^2}{72h_t^4} I_6^t)\ddot{\varphi}_{x,x}^t + (-\frac{h_c^2 h_t}{144} I_0^t + \frac{h_c^2}{9h_t} I_3^t - \frac{4h_c^2}{9h_t^4} I_6^t - \frac{h_c^2 h_b^2}{144} I_0^b$$
$$-\frac{h_c^2}{9h_b} I_3^b - \frac{4h_c^2}{9h_b^4} I_6^b)\ddot{w}_{0,xx}^c + (\frac{h_c^3 h_t^2}{288} I_0^t - \frac{h_c^3}{18h_t} I_3^t + \frac{2h_c^3}{9h_t^4} I_6^t$$
$$+\frac{h_c^3 h_b^2}{288} I_0^b + \frac{h_c^3}{18h_b} I_3^b + \frac{2h_c^3}{9h_b^4} I_6^b)\ddot{w}_{1,xx}^c + (-\frac{h_c^4 h_t^2}{576} I_0^t + \frac{h_c^4}{36h_t} I_3^t$$
$$-\frac{h_c^4}{9h_t^4} I_6^t - \frac{h_c^4 h_b^2}{576} I_0^b - \frac{h_c^4}{36h_b} I_3^b - \frac{h_c^4}{9h_b^4} I_6^b)\ddot{w}_{2,xx}^c + (\frac{h_c^2}{4} I_0^t$$
$$+\frac{h_c^2}{4} I_0^b + I_2^c)\ddot{w}_0^c + (-\frac{h_c^3}{8} I_0^t + \frac{h_c^3}{8} I_0^b + I_3^c)\ddot{w}_1^c + (\frac{h_c^4}{16} I_0^t$$
$$+\frac{h_c^4}{16} I_0^b + I_4^c)\ddot{w}_2^c = 0$$

In Eqs. (13-21), I_n^i (n = 0, 1, 2,3,4,5,6) (i = t, b, c) are the moments of inertia for the top and bottom face sheets as well as for the core and can be given as follows

$$I_n^i = \int_{-\frac{h_i}{2}}^{\frac{h_i}{2}} z_i^n \rho_i dz_i \quad \text{(i=t,b,c)}$$

The resultants of Eqs. (13-21) can be related to the total strains.

3. Analytical solution

The exact analytical solutions of Eqs. (13)-(21) existed for the simply supported sandwich beam with cross-ply face sheets. Both the face sheets were considered as a cross-ply laminated composite. The boundary conditions of a simply supported beam can be defined as

$$w_0(0,t) = w_0(L,t) = 0, \quad M_{xx}(0,t) = M_{xx}(L,t) = 0$$

As the above equations of motion (Eqs. (13)-(21)) are in space and time coordinates, generalized Galerkin's principle was used to reduce these equations to their temporal form. For multimode discretization, one may take

$$\begin{aligned}
&u_0^c = \sum_{i=1}^{N} a_i(t)\varphi_{ai}(x),\ u_1^c = \sum_{i=1}^{N} b_i(t)\varphi_{bi}(x),\\
&u_2^c = \sum_{i=1}^{N} c_i(t)\varphi_{ci}(x), u_3^c = \sum_{i=1}^{N} d_i(t)\varphi_{di}(x),\\
&\varphi_x^t = \sum_{i=1}^{N} e_i(t)\varphi_{ei}(x),\ \varphi_x^b = \sum_{i=1}^{N} f_i(t)\varphi_{fi}(x),\\
&w_0^c = \sum_{i=1}^{N} g_i(t)\varphi_{gi}(x),\ w_1^c = \sum_{i=1}^{N} l_i(t)\varphi_{li}(x),\\
&w_2^c = \sum_{i=1}^{N} m_i(t)\varphi_{mi}(x)
\end{aligned} \tag{22}$$

Here, N is a positive integer representing the number of modes taken in the analysis; $a_i, b_i, c_i, d_i, e_i, f_i, g_i, l_i$ and m_i are the generalized coordinates; and $\phi_{ai}, \phi_{bi}, \phi_{ci}, \phi_{di}, \phi_{ei}, \phi_{fi}, \phi_{gi}, \phi_{li}$ and ϕ_{mi} are the shape functions chosen to satisfy boundary conditions as many as possible. For the simply supported beam

$$\begin{aligned}
&\varphi_{ai}(x) = \cos(\frac{i\pi x}{L}),\ \varphi_{bi}(x) = \cos(\frac{i\pi x}{L}),\\
&\varphi_{ci}(x) = \cos(\frac{i\pi x}{L}),\ \varphi_{di}(x) = \cos(\frac{i\pi x}{L}),\\
&\varphi_{ei}(x) = \cos(\frac{i\pi x}{L}),\ \varphi_{fi}(x) = \cos(\frac{i\pi x}{L}),\\
&\varphi_{gi}(x) = \sin(\frac{i\pi x}{L}),\ \ \varphi_{li}(x) = \sin(\frac{i\pi x}{L}),\\
&\varphi_{mi}(x) = \sin(\frac{i\pi x}{L})
\end{aligned} \tag{23}$$

These shape functions satisfied all the boundary conditions.

The resulting equation of motion became

$$[M]\{\ddot{f}\} + [K]\{f\} - \beta P_{cr}\cos\theta t [H]\{f\} = 0 \tag{24}$$

where

$$(.) = d(.)/dt, \{f\} = \begin{Bmatrix} \{a_i\}^T, \{b_i\}^T, \{c_i\}^T, \{d_i\}^T, \{e_i\}^T \\ \{f_i\}^T, \{g_i\}^T, \{l_i\}^T, \{m_i\}^T \end{Bmatrix}^T$$

and

$$[K] = [K_1] - \alpha P_{cr}[H] - [K_f]$$

To solve the nonlinear eigenvalue problem, an iterative scheme was used (Sarma and Varadan 1983). First, the amplitude was set an equal to zero and was solved the resulting linear eigenvalue problem. The linear eigenvalues and eigenvectors were then used to obtain nonlinear coefficients. The eigenvalue problem was solved again - to obtain nonlinear eigenvalues and eigenvectors and the process repeated. It did not take too many times to get convergence of eigenvalues and eigenvectors.

4. Dynamic instability analysis

The periodic motion of the system is usually the boundary case of vibrations with unboundedly increasing amplitudes (Nayak *et al.* 2014). Therefore, it is important to study the dynamic instability of the system and determination of the boundaries of dynamic instability regions. Eq. (24) is a set of Mathieu type equations governing the instability behavior of the beam structure. For the given values of the three parameters α, β and Ω, the solution of this equation may be either bounded or unbounded. The spectrum of these values of parameters had unbounded solutions for some regions of the planes due to parametrically excited resonance. This phenomenon is known as dynamic instability and these regions are named as dynamic instability regions (DIRs). The boundaries of

DIRs were determined by the periodic solutions having the periods T and 2T according to Bolotin's approach. The instability region at the boundaries of the period 2T had great practical importance and hence, the solution of Eq. (24) was achieved by presenting the components {*f*} in trigonometric series form as follows

$$\{f\} = \sum_{i=1,3,5,\ldots}^{\infty} \left[\{a_i\} \sin\frac{i\Omega t}{2} + \{b_i\} \cos\frac{i\Omega t}{2} \right] \tag{25}$$

with period 2T,

$$\text{where } T = \frac{2\pi}{\Omega}$$

Here, $\{a_i\}$ and $\{b_i\}$ are vectors independent of the time t. The above equations were substituted in Eq. (24) and the sums of the coefficients of each sine and cosine terms were equated to zero which led to a series of algebraic equations for determining instability regions. The principal instability region corresponding to *i*=1 had practical significance and hence, the dynamic instability equation for this case yielded to

$$\left| [K_e] - \frac{\Omega^2}{4}[M] \pm 0.5P_t[H] \right| = 0 \tag{26}$$

where K_e and M are the stiffness matrix and mass matrix, respectively.

Eq. (26) was basically a generalized eigenvalue problem of the systems for the known values of α, β and P_{cr}. The two conditions under a plus and minus sign indicated two boundaries of the DIR. The eigenvalue problem was solved and the excitation frequencies Ω were obtained for the given values of α and β.

5. Results and discussion

In this section, some examples were considered and the obtained results were validated and discussed. The dynamic characteristics such as fundamental frequency and dynamic stability of the system were studied using various system parameters. A MATLAB code was developed for this purpose and to validate the developed code, the natural frequencies without considering the axial load were compared with those obtained from the previous literature. The results were validated with the recent theoretical and numerical results found in the literature. The agreement between the results was quite good.

Example 1: Free vibration of a sandwich beam with soft core

Since there were few researches about dynamic instability analysis of sandwich beams to validate the obtained results, the fundamental non-dimensional natural frequencies were calculated for the beam with simply supported boundary conditions and compared with the result of (Khdeir *et al.* 2016). The mechanical and geometrical properties of the sandwich beam are given in Table 1.

Table 1 Materials and geometrical properties of the sandwich beam (Khdeir *et al.* 2016)

Face sheet	E=10658 Mpa, G=4000 Mpa, ρ=1446 kg/m^3
Core	E_c =115 MPa, ρ=199 kg/m^3, ν=0.3
Geometry	$L = 254mm$, $h_t = h_b = 0.762mm$, $h_c = 12.7mm$, b=25.4mm

Table 2 Comparison of nondimensional natural frequencies ω for simply supported sandwich beam

Mode no.	Malekzadeh *et al.* 2015	ABAQUS	Present: Higher order theory	Difference (%)	Difference (%)
1	282.5	282.5	282.5	0.0	0.0
2	932.5	932.3	932.7	0.04	0.02
3	1697.6	1696.5	1697.6	0.06	0.0
4	2480	2476.7	2478.7	0.08	-0.05
5	3256.8	3249.6	3252.2	0.08	-0.14

Table 3 Materials and geometrical properties of the sandwich beam (Yang and Qiao 2005)

Face sheet	$E = 36$ GPa, ρ=4400 kg/m^3, ν=0.3
Core	$E_c = 0.05$ GPa, $G_c = 0.02$ GPa, ρ=52.06 kg/m^3, ν=0.3
Geometry	$L = 300mm$, $h_t = h_b = 0.5mm$, $h_c = 20mm$, b=20mm

Table 2 provides the comparison of the first five modal frequencies of vibration for the beam model, derived using the higher order beam theory and ABAQUS FE code, against the results from (Khdeir *et al.* 2016) The zigzag theory and experimental tests were used in (Khdeir *et al.* 2016). The natural frequencies were performed in ABAQUS/Standard software, which used a central difference rule to integrate the governing equations of motion explicitly. In this study, the face sheets and foam core were meshed using S8R elements, respectively. There was quite good agreement between the results.

Example 2: Free vibration analysis of a sandwich beam with isotropic core and face sheets

In this example, the free vibration analysis of a sandwich isotropic beam with SS B.Cs was performed. The properties of the model with the detailed geometry are presented in Table 3.

In Table 4, the results of the presented method for the first four natural frequencies are compared with those obtained by ABAQUS FE code and the ones presented in Frostig and Baruch (1994), Yang and Qiao(2005) and (Rahmani *et al.* 2009) which demonstrated good correspondence. Moreover, difference between the higher order beam theory results and the references (Frostig and Baruch 1994, Yang and Qiao 2005 and Rahmani *et al.* 2009) is presented in Table 4. There was quite good agreement between the results, and only little difference was observed between them.

Table 4 Comparison of the natural frequencies of sandwich beam

Mode no.	Frostig and Baruch (1994)	Yang,Qiao (2005)	(Rahmani *et al.*2009)	ABAQUS	Present Difference (%)	Higher order theory	Difference (%)
1	325.98	325.98	326.39	323.57	0.02	323.63	-0.72
2	825.30	824.96	826.62	814.65	-0.05	814.21	-1.3
3	1310.38	1308.90	1311.84	1294.3	-0.2	1291.4	-1.3
4	1779.83	1776.11	1780.25	1763.8	-0.4	1755.4	-1.2

Table 5 Materials and geometrical properties of the sandwich beam (Khdeir *et al*. 2016)

Face sheet	Cross-ply (graphite/epoxy orthotropic laminate $(0^\circ/90^\circ)$: $E_1=131GPa, E_2=E_3=10.34$ GPa, $G_{12}=G_{13}=6.895GPa, G_{23}=6.205GPa$ $v_{12}=v_{13}=0.22, v_{23}=0.49, \rho=1627\,kg/m^3$
Core	Isotropic material: $E=6.90$ MPa, G=3.45 MPa, ρ=97 kg/m^3, ν=0
Geometry	Core/face thickness ratio: ($L/h=10$), $h_c/h_i=10:1$, $(i=b,t)$.

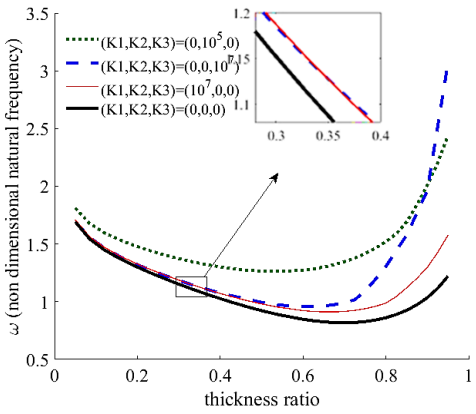

Fig. 2 Variation of the nondimensional natural frequency of the sandwich beam with the core thickness for $L/h=10$, $\alpha=0.5$ and $h=0.012m$

Example3: Dynamic instability analysis of a composite-faced sandwich beam with soft core on elastic foundation

In this example, the dynamic instability analysis of a sandwich beam with SS B.Cs was performed. The properties of the model with the detailed geometry are presented in Table 5. The first natural frequencies of the sandwich beam with different foundation's modulus and different thickness ratios are shown in Fig. 2.

It can be seen in the picture that with the increase of the thickness ratio (h_c/h), the frequencies was first declined but then increased gradually. It was because in the first period, the increase of the ratio (h_c/h) reduced the stiffness of the sandwich beam, but when exceeding a critical value, the mass matrix of the beam played a major role. As shown

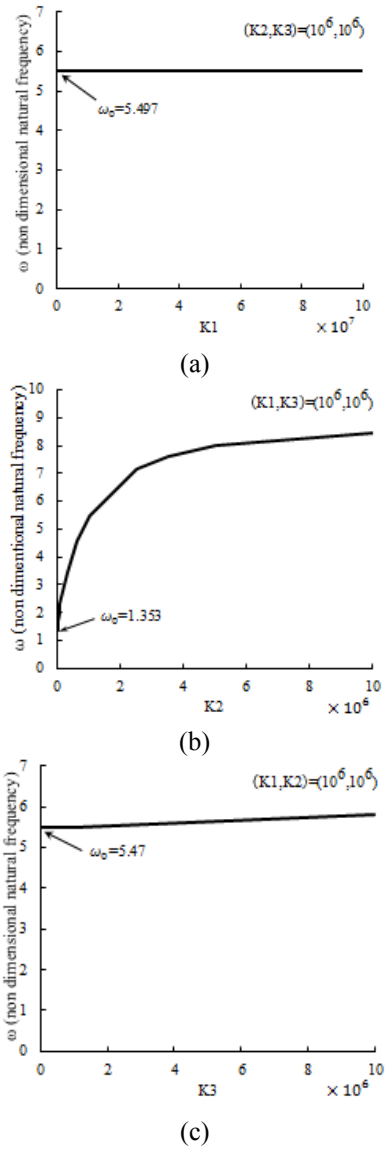

Fig. 3 The effects of (a) Winkler's coefficient (K1) (b) Pasternak's coefficient (K2) (c) nonlinear's coefficient (K3) with $L/h=10$ on the nondimensional fundamental natural frequency of sandwich beam

in Fig. 2, According to this example, in the values of $h_c/h<0.35$, K3 had the least effect on the variation of the natural frequency and in the values of $h_c/h>0.35$; K1 had the lowest effect on the natural frequency. In the values of $h_c/h>0.92$, K3 had the highest effect and in the values of $h_c/h<0.92$, K2 had the highest effect on the variation of the natural frequency.

Figs. 3(a)-(c) respectively show the effects of linear (K1), shear (K2) and nonlinear (K3) coefficients of elastic foundation on the first natural frequencies of the sandwich beam. It was found that the natural frequency increased with the coefficients of elastic foundation. This was due to the fact that the foundation increased the effective stiffness of the beam, which made the beam more stable. It was observed that the coefficient of shear stiffness (K2) had the greatest effect on the natural frequency. Fig. 3 also shows

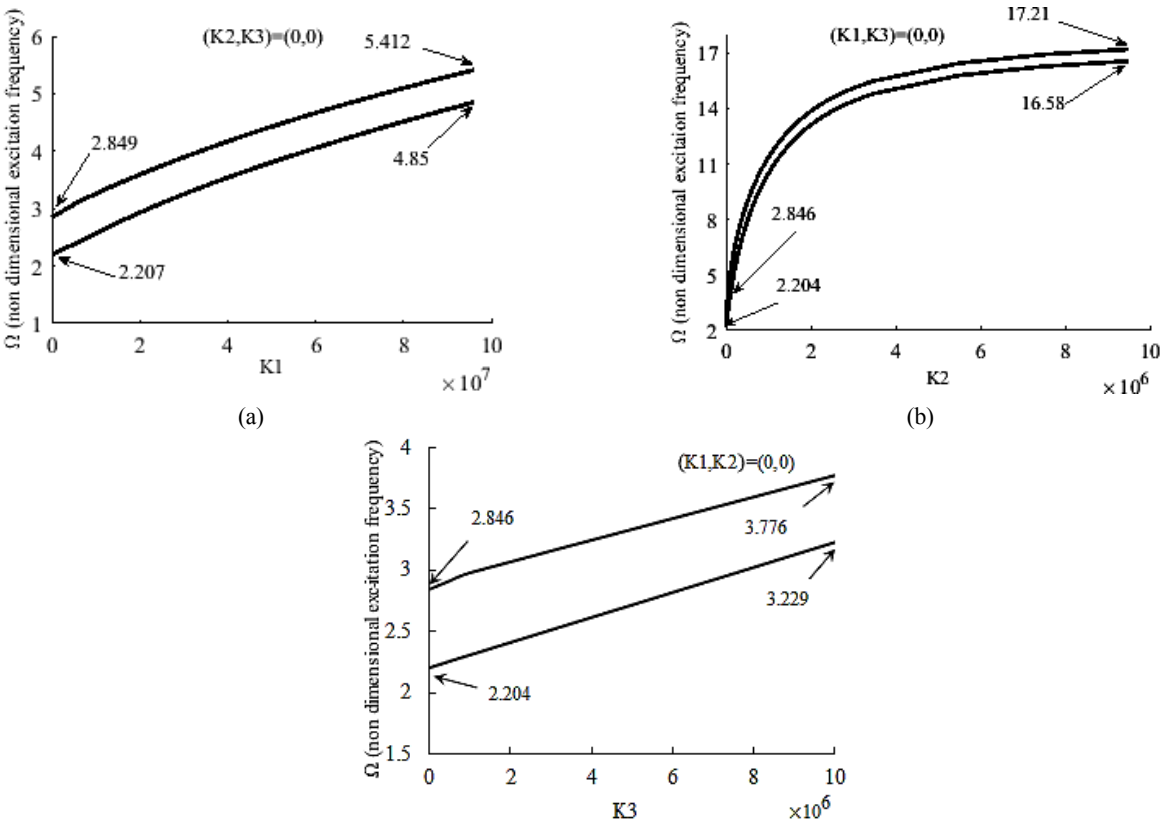

Fig. 4 Effect of the coefficients of elastic foundation on nondimensional fundamental excitation frequency of sandwich beam with ($L/h=10$), $\alpha=0$ and $\beta=0.5$

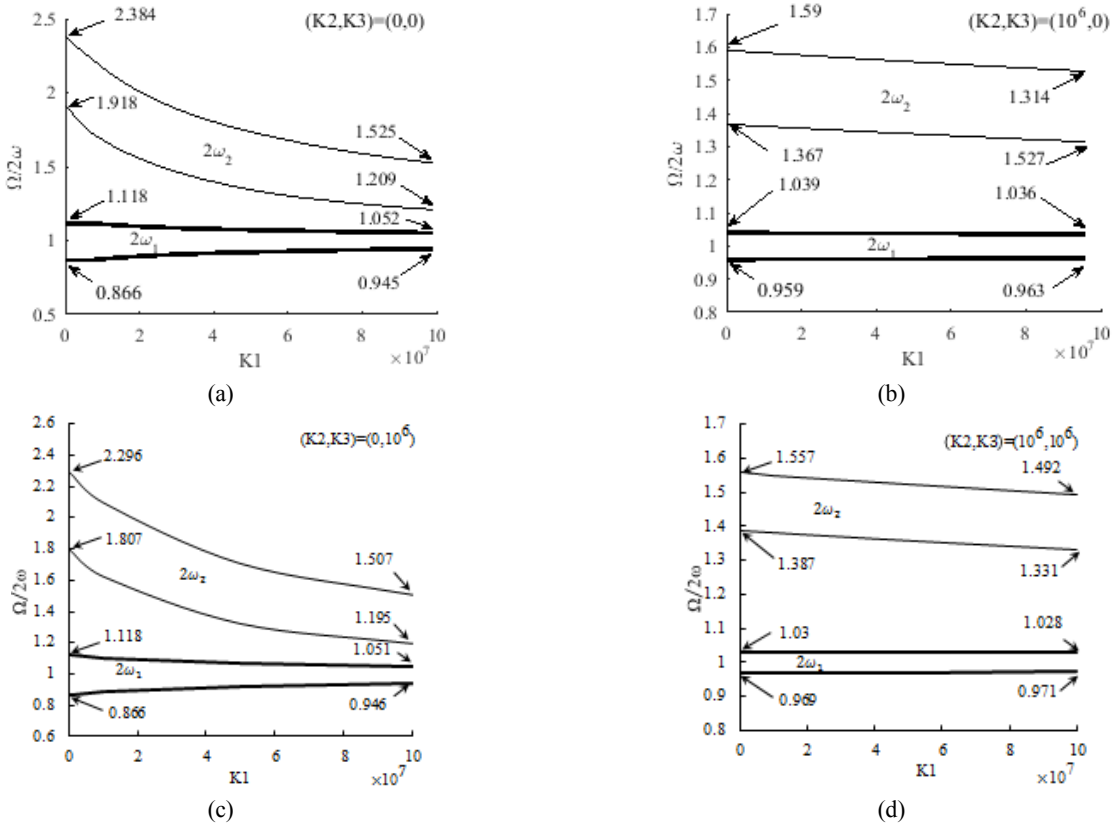

Fig. 5 Effect of the linear coefficient (K1) on the dynamic instability regions of sandwich beam with $L/h=10$, $\alpha=0$, and $\beta=0.5$

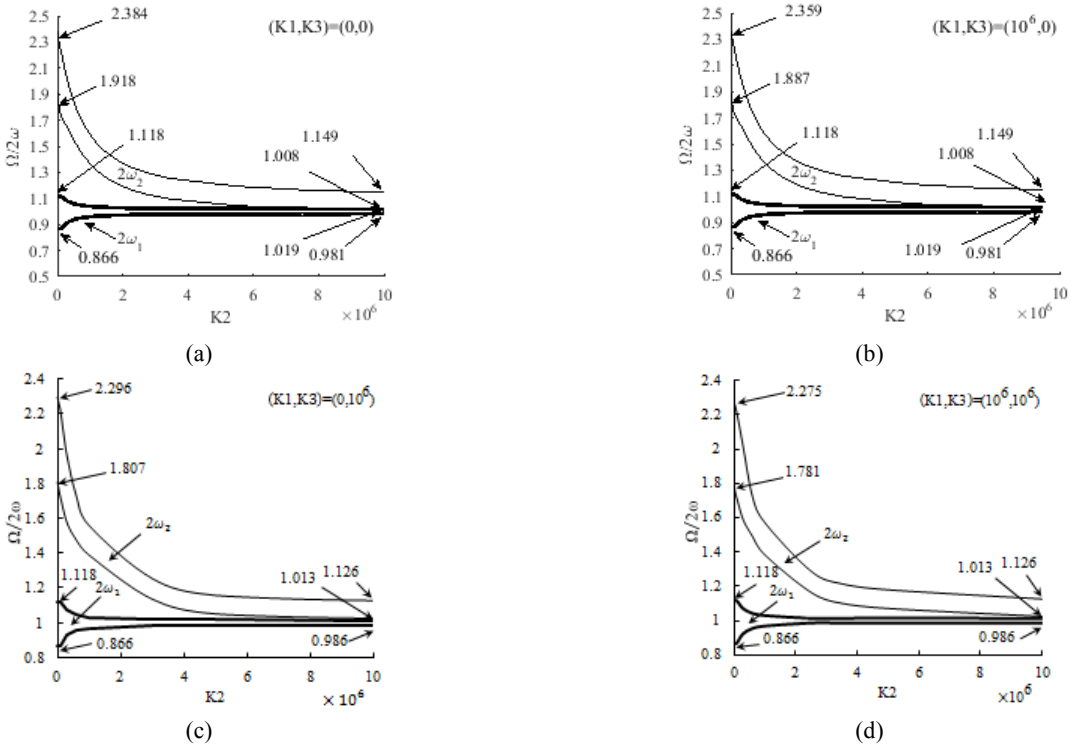

Fig. 6 Effect of the shear stiffness coefficient (K2) on the dynamic instability regions of sandwich beam with $L/h=10$, $\alpha=0$, and $\beta=0.5$

that as K2 was increased, natural frequencies variations were reduced. However, K2 changed the natural frequency nonlinearly and K1 and K3 had almost linear variations of natural frequencies. Further, the effect of elastic foundation was verified on the dynamic stability analysis of the sandwich beam. The dynamic instability regions for the nondimensional excitation frequencies are obtained via varying the coefficients of foundation from 0 to 10^7 and 10^8 while assuming the L/h ratio as ten; the instability regions are featured in Fig. 4 and the static factor of load was considered as 0. The figure signified that by increasing the coefficients of foundation, the onset of instability occurred later with narrower instability regions. By increasing the coefficients of foundation, the excitation frequency was decreased and the sandwich beam was stable at higher excitation frequencies, as shown in Fig. 4. Also, by increasing the coefficients of K1, K2, and K3, the range of excitation frequencies, which is the cause of instability, decreased.

Fig. 5 shows that the increase of K1 resulted in a narrower instability region and a more stable sandwich beam. Moreover, K3 had a negligible effect on the instability of sandwich beam compared to K2. Also, by increasing K2, the instability region became narrower and the sandwich beam was more stable as shown in Fig. 6. Furthermore, K1 had less effect on reducing instability of sandwich beam compared to K3. By increasing K3, the instability of sandwich beam has been reduced if K3, alone, or with K1 is considered as shown in Fig. 7. Also, the variations of K3 have no effect on the dynamic instability of the beam if K1, K2, and K3 are considered.

The above results can be interpreted ($h_c/h=0.833$) according to the results of the Fig. 2.

Fig. 8 shows the effect of the elastic foundation on the instability regions of the sandwich beam for two frequency modes. Similar results were obtained as shown in Figs. 5-7. It was observed that the instability regions of the beam resting on the foundation were shifted toward the axis of the dynamic load factor except the first instability region and had lower width as the foundation modulus increased. This was due to the fact that the foundation increased the effective stiffness matrix of the beam, which made the beam more stable. The shaded area is an unstable region for $\beta=0.5$, as shown in Fig. 8.

The variation of the fundamental natural frequency of the beam loaded with static buckling factor with L/*h* = 10 is shown in Fig. 9. The natural frequency of the beam decreased with increase of the static load factor, whereas the natural frequency increased with increase of the coefficients of foundation. Also, by increasing the static load factor, the difference of the natural frequencies decreased in different conditions of the elastic foundation.

Fig. 10(a) shows the effect of the static load factor on the first mode excitation frequency of the sandwich beam. It was found that the excitation frequencies decreased with the static load factor. It was also observed that the shaded area was an unstable region for $\beta=0.5$. To validate the instability regions, one may numerically solve Eq. (23) for a wide range of system parameters. Although actually checked for several points, here, the time response curves (Figs. 11-14) were plotted for the two points marked A and B corresponding to the system parameters in Fig. 10(b).

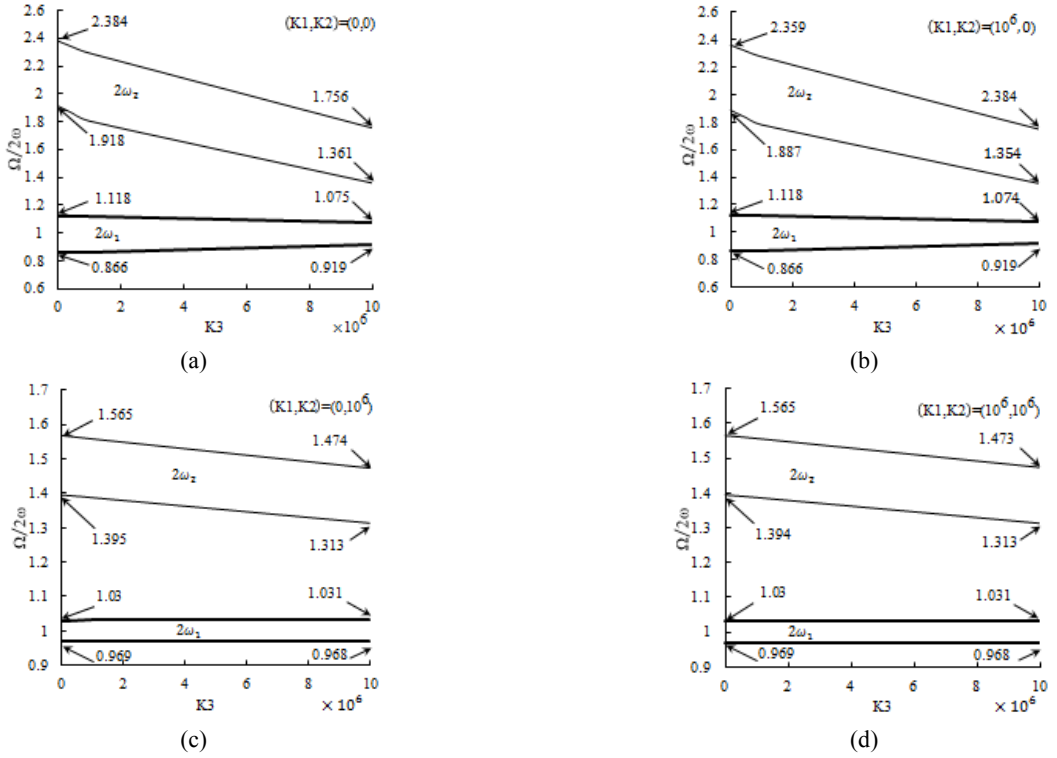

Fig. 7 Effect of the nonlinear coefficient (K3) on the dynamic instability regions of sandwich beam with $L/h=10$, $\alpha=0$, and $\beta=0.5$

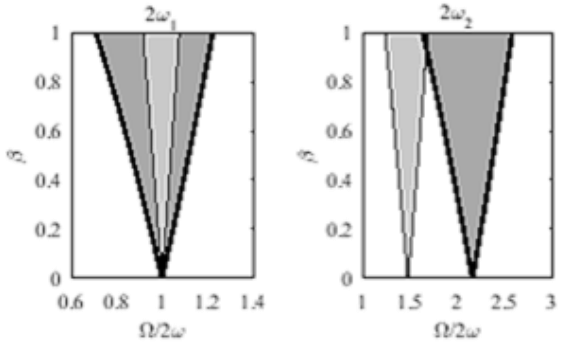

Fig. 8 Instability regions of sandwich beam for the first and second modes: (-) Beam without the elastic foundation, (-) beam on the foundation with (K1, K2, K3) = (10^6 , 10^6 , 0) for $\alpha=0$ with $L/h=10$

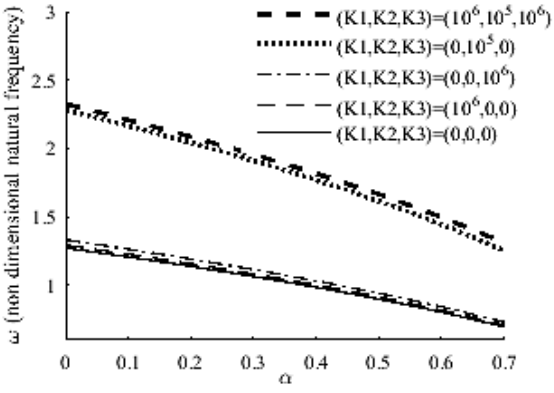

Fig. 9 Variation of the nondimensional natural frequency of the sandwich beam with the static buckling factor for $L/h=10$

As seen from Fig. 10(a), the width of the instability regions increased with an increase in the static load factor. The first instability regions are presented for the thick sandwich beam in Fig. 10(b), where the parametric ratio $\Omega/2\omega_1$ was plotted with respect to the static load factor α for the fixed values of the dynamic parameter β. The parametric ratio was obtained by dividing the parametric resonance frequency Ω resulting from Eq. (25) by $2\omega_1$, the natural frequency of the loaded beam obtained by neglecting the harmonic term in Eq. (23). The quantity $P_t=\beta P_{cr}$ defined the amplitude of the dynamic component of the compressive force, whereas the static parameter $P_0=\alpha P_{cr}$ defined the magnitude of the static component of the compressive force (Eq. (1)). As seen from Fig. 10(b), the width of the instability regions increased with an increase in the static and dynamic loads. Fig. 10(b) emphasizes that a sandwich beam resting on the nonlinear elastic base is more stable than the sandwich beam without elastic foundation. By increasing the static buckling coefficient, the dynamic stability of the beam on the foundation was increased compared to the beam without the foundation For example, for the system parameters of the point marked A, ($\alpha=0.6$, $\beta=0.5$) and ($\alpha=0.6$, $\beta=0.25$) clearly corresponding to $\Omega/2\omega=0.644$, the system was found to be stable and, for the point marked B, ($\alpha=0.6$, $\Omega/2\omega=0.841$) corresponding to $\beta=0.5$, the system was found to be unstable. Similarly, for $\beta=0.25$ from Fig. 10(b), the system was found to be stable.

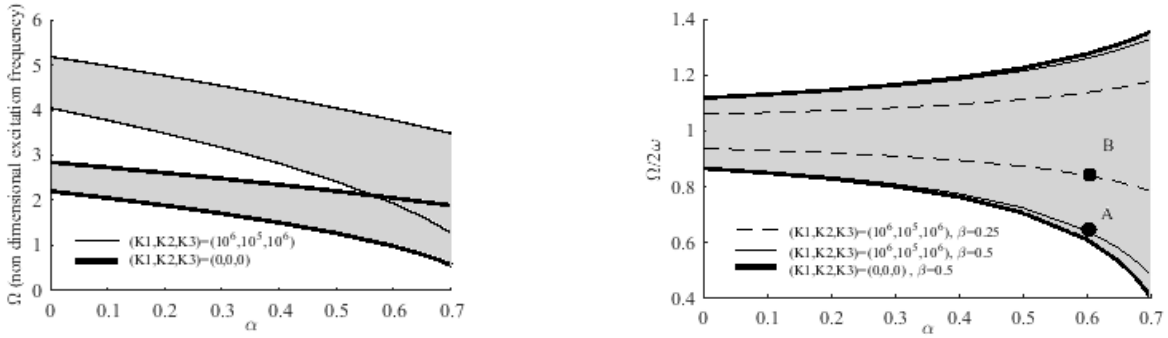

(a) (b)

Fig. 10 (a) Variation of the nondimensional excitation frequency of the sandwich beam with the static buckling factor for $\beta = 0.5$ and $L/h = 10$; (b) Variation of the parametric ratio of the sandwich beam with the static buckling factor for $\beta = 0.25$ and $\beta = 0.5$ with $L/h = 10$

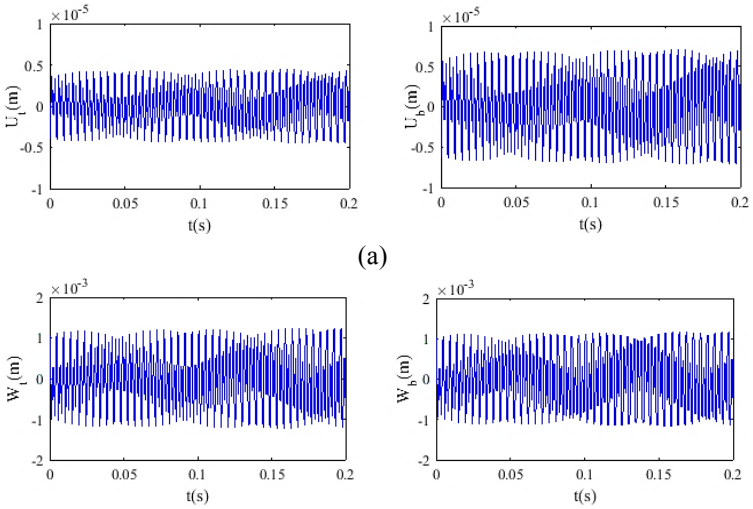

(a)

(b)

Fig. 11 Time response of the soft cored sandwich beam at $\beta = 0.5$ (at the point marked A in Fig. 10(b)): (a) Response of core and face sheets in the horizontal direction (U), (b) Response of core and face sheets in the vertical direction (W) for $\alpha = 0.6$ with $L/h = 10$ and $(K1, K2, K3) = (10^6, 10^5, 10^6)$

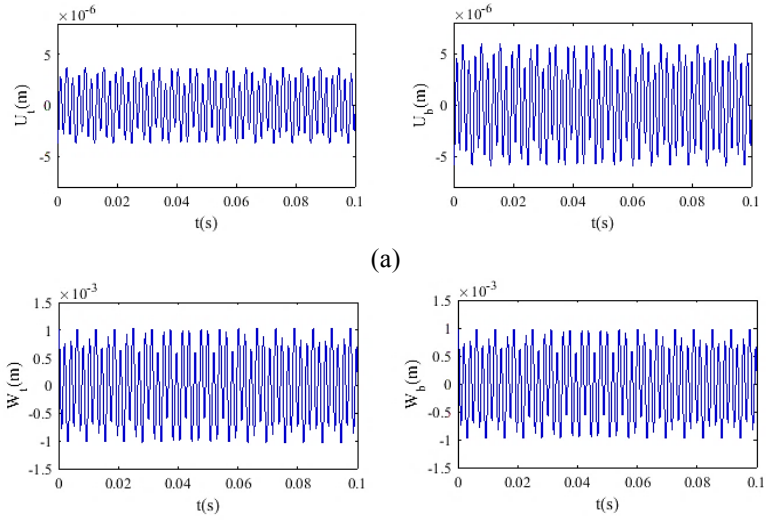

(a)

(b)

Fig. 12 Time response of the soft cored sandwich beam at $\beta = 0.25$ (at the point marked A in Fig. 10(b)): (a) Response of core and face sheets in the horizontal direction (U), (b) Response of core and face sheets in the vertical direction (W) for $\alpha = 0.6$ with $L/h = 10$ and $(K1, K2, K3) = (10^6, 10^5, 10^6)$

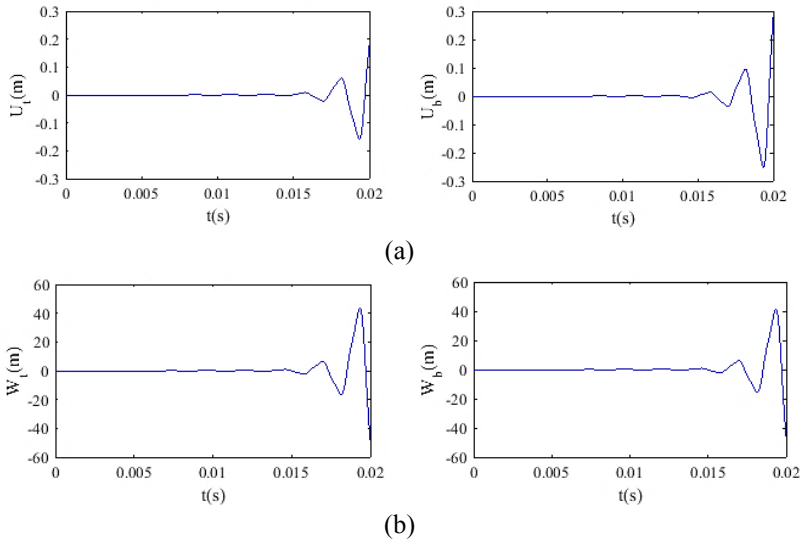

Fig. 13 Time response of the soft cored sandwich beam at $\beta = 0.5$ (at the point marked B in Fig. 10(b)): (a) Response of core and face sheets in the horizontal direction (U), (b) Response of core and face sheets in the vertical direction (W) for $\alpha = 0.6$ with $L/h = 10$ and $(K1, K2, K3) = (10^6, 10^5, 10^6)$.

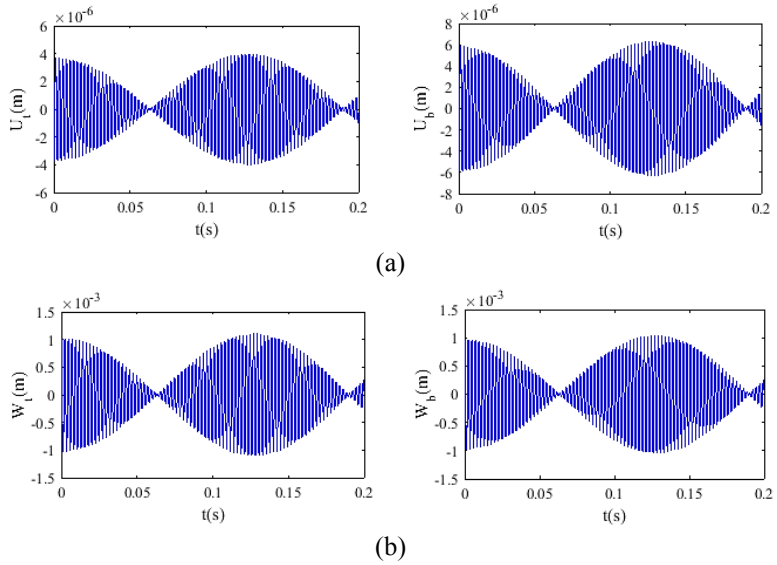

Fig. 14 Time response of the soft cored sandwich beam at $\beta = 0.25$ (at the point marked B in Fig. 10(b)): (a) Response of core and face sheets in the horizontal direction (U), (b) Response of core and face sheets in the vertical direction (W) for $\alpha = 0.6$ with $L/h = 10$ and $(K1, K2, K3) = (10^6, 10^5, 10^6)$.

This was in good agreement with the observations in Fig. 10(b). It may be noted that obtaining the instability plot by solving Eq. (24) requires a huge memory space and computational time. Hence, the developed simplified equation may be used for plotting the instability plot.

6. Conclusions

In this work, the governing equations of motion of a soft-cored symmetric sandwich beam subjected to periodic axial end load resting on the nonlinear elastic foundation was derived using a higher-order beam theory. These equations were reduced to that of a Mathieu-Hill's type of equations, which was used to find the parametric instability regions by applying the modified Bolotin's method. A code was developed and validated by comparing the obtained results with those found in the earlier literature. The instability regions were plotted for simply supported conditions for the sandwich beam. Moreover, these regions were plotted for systems with principal parametric resonances of different types. The correctness of the instability regions was verified by finding the time response from the temporal equation of motion and they were found to be in good agreement. The developed equations will have a range of applications in finding vibration attenuation

methods and increasing the system dynamic stability on the elastic foundation in a sandwich beam when subjected to periodic axial loading.

Validation of the evaluated results with various analytical and FEM solutions was performed. The well agreed results with the compared results, excellent mesh convergence, and accurate analysis of dynamic instability behavior ensured that the present theory was quite efficient to handle the dynamic stability analysis of sandwich beams.

The variation of fundamental natural and excitation frequency for different system parameters such as coefficients of foundation, dynamic and static load factor and core thickness was investigated. The natural frequency of the sandwich beam increased with coefficients of foundation. It was found that the foundation enhanced the stability of the sandwich beam. The instability region became wider with increasing values of the dynamic load and static buckling factor.

References

Bennai, R., Hassen, A.A. and Tounsi, A. (2015), "A new higher-order shear and normal deformation theory for functionally graded sandwich beams", *Steel Compos. Struct.*, **19**(3), 521-546. https://doi.org/10.12989/scs.2015.18.3.793.

Bolotin, V.V. (1956), *The Dynamic Stability of Elastic Systems*, Gostekhizdat, Moscow, Russia.

Bose, S., Chugh, P. and Gupta, A. (2012), "Effect of Elastic Foundation and Damping on Parametric Instability of Beams", *International Conference on Structural and Civil Engineering*, Hong Kong, July.

Bremen, H.F., Sokolinsky, V.S., Lavoie, J.A. and Nutt, S.R. (2001), "Experimental and analytical study of natural vibration modes of soft-core sandwich beams", *Proceedings of the 46th International SAMPE Symposium and Exhibition*, CA, Long Beach, USA.

Cunedioglu, Y. (2015), "Free vibration analysis of edge cracked symmetric functionally graded sandwich beams", *Struct. Eng. Mech.*, **56**(6), 1003-1020. https://doi.org/10.12989/sem.2015.56.6.1003.

Demir, E. (2017), "Vibration and damping behaviors of symmetric layered functional graded sandwich beams", *Struct. Eng. Mech.*, **62**. (6), 771-780. https://doi.org/10.12989/sem.2017.62.6.771.

Doddamani, M.R., Kulkarni, and S.M. Kishore, (2011), "Behavior of sandwich beams with functionally graded rubber core in three point bending", *Polym. Compos.*, **32**, 1541-1551. https://doi.org/10.1002/pc.21173.

Dwivedy, S.K., Sahu, K.C. and Babu. S. (2007), "Parametric instability regions of three layered soft-cored sandwich beam using higher order theory", *J. Sound Vib.*, **304**, 326-344. https://doi.org/10.1016/j.jsv.2007.03.016.

Fattahi, A.M and Safaei, B. (2017), "Buckling analysis of CNT-reinforced beams with arbitrary boundary conditions", *Microsyst. Technol.,* **23**(10), 5079-5091. https://doi.org/10.1007/s00542-017-3345-5.

Frostig, Y. (1998), "Buckling of sandwich panels with flexible core—high order theory", *J. Solid Struct.*, **35** (3-4), 183-204. https://doi.org/10.1016/S0020-7683(97)00078-4.

Frostig, Y. and Baruch, M. (1990), "Bending of sandwich beams with transversely flexible core", *AIAA J.*, **28**(3), 523-531. https://doi.org/10.2514/3.10423.

Frostig, Y. and Baruch, M. (1994), "Free vibrations of sandwich beams with a transversely flexible core: A higher order approach", *J. Sound Vib.*, **176**(2), 195-208. https://doi.org/10.1006/jsvi.1994.1368.

Frostig, Y. and Baruch, M. (1996), "Localized load effects in high-order bending of sandwich panels with flexible core," *J. Eng. Mech.*, **122**(11), 1069-1076. https://doi.org/10.1061/(ASCE)0733-9399(1996)122:11(1069).

Frostig, Y. and Shenar, Y. (1995), "High-order bending of sandwich beams with a transversely flexible core and unsymmetrical laminated composite skins", *Compos. Eng.*, **5**(4), 405-414. https://doi.org/10.1016/0961-9526(95)93440-7.

Frostig, Y. and Thomsen, O.T. (2004), "Higher-order free vibration of sandwich panel with a flexible core", *J. Solid Struct.*, **41**, 1697-1724. https://doi.org/10.1016/j.ijsolstr.2003.09.051.

Ghosh, R., Dharmavaram, S., Ray, K. and Dash, P. (2005). "Dynamic stability of a viscoelastically supported sandwich beam", *Struct. Eng. Mech.*, **19**(5), 503-517. https://doi.org/10.12989/sem.2005.19.5.503.

Huang, Z.C., Qin, Z. and Chu, F. (2015), "Vibration and damping characteristics analysis of viscoelastic sandwich beams based on the shear dissipating energy assumption", *J. Vib. Shock*, **34**. https://doi.org/10.13465/j.cnki.jvs.2015.07.029.

Huang, Z., Qin, Z. and Chu, F. (2015), "A comparative study of finite element modeling techniques for dynamic analysis of elastic-viscoelastic-elastic sandwich structures", *J. Sandwich Struct. Mater.*, **18**(5), 531-551. https://doi.org/10.1177/1099636215623091.

Jam, E.J., Eftari, B. and Taghavian, S.H. (2010), "A new improved high-order theory for analysis of free vibration of sandwich panels", *Polym. Compos.*, **31**(12), 2042-2048. https://doi.org/10.1002/pc.21002.

Kar, R.C. and Sujata, T. (1991), "Dynamic stability of a tapered symmetric sandwich beam", *Comput. Struct.*, **40**, 1441-1449. https://doi.org/10.1016/0045-7949(91)90414-H.

Khalili, S.M.R., Kheirikhah, M.M. and Malekzadeh Fard, K. (2015), "Buckling analysis of composite sandwich plates with flexible core using improved high-order theory", *Mech. Adv. Mater. Struct.*, **22**(4), 233-247. https://doi.org/10.1080/15376494.2012.736051.

Khdeir, A.A. and O. J. Aldraihem, O.J. (2016), "Free vibration of sandwich beams with soft core", *Compos. Struct.*, **154**, 179-189. https://doi.org/10.1016/j.compstruct.2016.07.045.

Kheirikhah, M.M., Khalili, S.M.R. and Malekzadeh Fard, K. (2011), "Biaxial buckling analysis of soft-core composite sandwich plates using improved high-order theory", *European J. Mech. A Solids*, **31**(1), 54-66. https://doi.org/10.1016/j.euromechsol.2011.07.003.

Liu, Q. and Zhao, Y. (2006), "Natural frequency analysis of a sandwich panel with soft core based on a refined shear deformation model", *Compos. Struct.*, **72**, 364-374. https://doi.org/10.1016/j.compstruct.2005.01.006.

Malekzadeh Fard, K. (2014), "Higher order free vibration of sandwich curved beams with a functionally graded core", *Struct. Eng. Mech.*, **49**(5), 537-554. https://doi.org/10.12989/sem.2014.49.5.537.

Malekzadeh Fard, K., Livani, M., veisi, A. and Gholami, M. (2011), "Improved high-order bending analysis of double curved sandwich panels subjected to multiple loading conditions", *Lat. Am. J. Solids Struct.,* **11**(9), 1591-1614. http://dx.doi.org/10.1590/S1679-78252014000900006.

Malekzadeh, K., Khalili, A.M.R. and gorgabad, A.V. (2015), "Dynamic response of composite sandwich beams with arbitrary functionally graded cores subjected to low-velocity impact", *Mech. Adv. Mater. Struct.*, **22**, 605-618. https://doi.org/10.1080/15376494.2013.828814.

Malekzadeh, K., Khalili, M.R. and Mittal, R.K. (2005), "Local and global damped vibrations of plates with a viscoelastic soft flexible core: An improved high-order approach", *J. Sandwich Struct. Mater.*, **7**(5), 431-456.

https://doi.org/10.1177/1099636205053748.
Malekzadeh, K., Khalili, S.M.R. and Gorgabad, A.V. (2015), "Dynamic response of composite sandwich beams with arbitrary functionally graded cores subjected to low-velocity impact", *Mech. Adv. Mater. Struct.*, **22**, 605-618. https://doi.org/10.1080/15376494.2013.828814.
Mohanty, S.C., Dash, R.R. and Rout, T. (2010), "Static and dynamic analysis of a functionally graded Timoshenko beam on Winkler's elastic foundation", *J. Eng. Res. Studies*, **241**, 2698-2715. https://doi.org/10.1142/S0219455412500253.
Moradi-Dastjerdi, R. and Momeni-Khabisi, H. (2018), "Vibrational behavior of sandwich plates with functionally graded wavy carbon nanotube-reinforced face sheets resting on Pasternak elastic foundation", *J. Vib. Control*, **24**(11), 2327-2343. https://doi.org/10.1177/1077546316686227.
Nayak, B., Dwivedy, S.K. and Murthy, K.S.R.K. (2014), "Dynamic stability of a rotating sandwich beam with magnetorheological elastomer core", *European J. Mech., A/Solids*, **47**,143-145. https://doi.org/10.1016/j.euromechsol.2014.03.004.
Patel, B.P., Ganapathi, M., Prasad, K.R. and Balamurugan, V. (1999), "Dynamic instability of layered anisotropic composite plates on elastic foundations", *Eng. Struct.*, **21**, 985-995. https://doi.org/10.1016/S0141-0296(98)00063-7.
Petras, A. and Sutcliffe, M.P.F. (1999), "Indentation resistance of sandwich beams", *Composite Structures*, **46**(4), 413-424. https://doi.org/10.1016/S0263-8223(99)00109-9.
Pourasghar, A. and Chen, Z. (2016), "Thermoelastic response of CNT reinforced cylindrical panel resting on elastic foundation using theory of elasticity", *Compos. Part B Eng.*, **99**, 436-444. https://doi.org/10.1016/j.compositesb.2016.06.028.
Pourasghar, A. and Chen, Z. (2019), "Effect of hyperbolic heat conduction on the linear and nonlinear vibration of CNT reinforced size-dependent functionally graded microbeams", *J. Eng. Sci.,* **137**, 57-72. https://doi.org/10.1016/j.ijengsci.2019.02.002.
Pourasghar, A. and Kamarian, S. (2013), "Dynamic stability analysis of functionally graded nanocomposite non-uniform column reinforced by carbon nanotube", *J. Vib. Control*, 1-10. https://doi.org/10.1177/1077546313513625.
Pourasghar, A. Homauni, M, and Kamarian, S. (2015), "Differential quadrature based nonlocal flapwise bending vibration analysis of rotating nanobeam using the eringen nonlocal elasticity theory under axial load", *Polym. Compos.*, **37**(11), 3175-3180. https://doi.org/10.1002/pc.23515.
Pradhan, M., Mishra, M.K. and Dash, P.R. (2016), "Free vibration analysis of an asymmetric sandwich beam resting on a variable Pasternak foundation", *Procedia Eng.*, **144**, 116-123. https://doi.org/10.1016/j.proeng.2016.05.014.
Qin, Z., Chu, F. and Zu, J. (2017), "Free vibrations of cylindrical shells with arbitrary boundary conditions: A comparison study", *J. Mech. Sci.*, **133**, 91-99. https://doi.org/10.1016/j.ijmecsci.2017.08.012.
Qin, Zh, Pang, X, Safaei, B. and Chu, F. (2019), "Free vibration analysis of rotating functionally graded CNT reinforced composite cylindrical shells with arbitrary boundary conditions" *J. Mech. Sci.*, **220**, 847-860. https://doi.org/10.1016/j.compstruct.2019.04.046.
Qin, Zh, Yang, Zh, Zu, J, and Chu, F. (2018), "Free vibration analysis of rotating cylindrical shells coupled with moderately thick annular plates", *J. Mech. Sci.*, **142-143**, 127-139. https://doi.org/10.1016/j.ijmecsci.2018.04.044.
Rahmani, O., Khalili, S.M.R., Malekzadeh, K. and Hadavinia, H. (2009), "Free vibration analysis of sandwich structures with a flexible functionally graded syntactic core", *Compos. Struct.*, **91**(2), 229-235. https://doi.org/10.1016/j.compstruct.2009.05.007.
Ray, K. and Kar, R. (1995), "Parametric instability of a sandwich beam with various boundary conditions", *Comput. Struct.*, **55**, 857-870. https://doi.org/10.1016/0045-7949(94)00427-5.
Ray, K. and Kar, R.C. (1996), "Parametric instability of multi-layered sandwich beams", *J. Sound Vib.*, **193**, 631-644. https://doi.org/10.1006/jsvi.1996.0305.
Reddy, J.N. (2004), *Mechanics of Laminated Composite Plates and Shells,Theory and Analysis*, 2nd ed., CRC Press, Florida, USA.
Safaei, B, Moradi-Dastjerdi, R. and Chu, F. (2018), "Effect of thermal gradient load on thermo-elastic vibrational behavior of sandwich plates reinforced by carbon nanotube agglomerations", *Compos. Part B Eng.*, **192**, 28-37. https://doi.org/10.1016/j.compstruct.2018.02.022.
Safaei, B, Moradi-Dastjerdi, R, Qin, Z. and Chu, F. (2018), "Frequency-dependent forced vibration analysis of nanocomposite sandwich plate under thermo-mechanical loads", *Compos. Part B Eng.*, **161**, 44-54. https://doi.org/10.1016/j.compositesb.2018.10.049.
Sarma, B.S. and Varadan, T.K. (1983), "Lagrange-type formulation for finite element analysis of non-linear beam vibrations", *J. Sound Vib.*, **86**(1), 61-70. https://doi.org/10.1016/0022-460X(83)90943-4.
Smyczynski, M., and Magnucka, E. (2018), "Stability of five layer sandwich beams - A nonlinear hypothesis", *Steel Compos. Struct.,* **28**(6), 671-679. https://doi.org/10.12989/scs.2018.28.6.671.
Sokolinsky, V.S. and Nutt, S.R. (2004), "Consistent higher-order dynamic equations for soft-core sandwich beams", *AIAA J.*, **42**(2), 374-382.
Sokolinsky, V.S., Bremen, H.F., Lavoie, J.A. and Nutt, S.R. (2004), "Analytical and experimental study of free vibration response of soft-core sandwich beams", *J. Sandwich Struct. Mater.*, **6**(3), 239-261. https://doi.org/10.1177/1099636204034634.
Tornabene, F., Fantuzzi, N., Viola, E. and Reddy, J.N. (2014), "Winkler-Pasternak foundation effect on the static and dynamic analyses of laminated doubly-curved and degenerate shells and panels", *Compos. Part B,* **57**, 269-296. https://doi.org/10.1016/j.compositesb.2013.06.020.
Yang, M. and Qiao, P. (2005), "Higher-order impact modeling of sandwich structures with flexible core", *J. Solid Struct.*, **42**(20), 5460-5490. https://doi.org/10.1016/j.ijsolstr.2005.02.037.
Zenkour, A.M. (2005), "A comprehensive analysis of functionally graded sandwich plates: Part 1 - deflection and stresses", *J. Solid Struct.*, **42**(18-19), 5224-5242. https://doi.org/10.1016/j.ijsolstr.2005.02.015.
Zenkour, A.M. (2005), "A comprehensive analysis of functionally graded sandwich plates: part 2-deflection and stresses", *J. Solid Struct.*, **42**, 5224-5242. https://doi.org/10.1016/j.ijsolstr.2005.02.016.

PL